ornl

ORNL/Sub/85-97343/2
(RSI-0305)

OAK RIDGE
NATIONAL
LABORATORY

MARTIN MARIETTA

Thermomechanical Properties of Selected Shales

Francis D. Hansen
Timothy J. Vogt

OPERATED BY
MARTIN MARIETTA ENERGY SYSTEMS, INC.
FOR THE UNITED STATES
DEPARTMENT OF ENERGY

DISCLAIMER

Printed in the United States of America. Available from
National Technical Information Service
U.S. Department of Commerce
5285 Port Royal Road, Springfield, Virginia 22161
NTIS price codes—Printed Copy: A06; Microfiche A01

ORNL/Sub--85-97343/2

DE88 001509

THERMOMECHANICAL PROPERTIES OF SELECTED SHALES

Francis D. Hansen
Timothy J. Vogt

DATE OF ISSUE — AUGUST 1987

Prepared by the Staff of
RE/SPEC, Inc.
P. O. Box 725
Rapid City, South Dakota 57709
under
Subcontract No. 12X-97343

for

OAK RIDGE NATIONAL LABORATORY
Oak Ridge, Tennessee 37831
operated by
MARTIN MARIETTA ENERGY SYSTEMS, INC.
for the
U.S. DEPARTMENT OF ENERGY
under Contract No. DE-AC05-840R21400

FOREWORD

This report summarizes thermomechanical test results obtained by testing several shales from the United States. The experimental work undertaken and reported here is part of an ongoing evaluation of various rock types as potential hosts for a geologic repository. The purpose for conducting particular experiments on shales is to provide baseline thermomechanical properties which can be used to evaluate shale as a host medium, as well as to differentiate between shale types.

Several persons have contributed to this report. Dr. Thomas F. Lomenick of ORNL was instrumental in several phases of this program including core acquisition, distribution of cores, and planning and implementation of tests. Dr. Arlo F. Fossum provided leadership of the RE/SPEC effort, and his encouragement and advice are gratefully acknowledged. The experiments were conducted by several individuals. Mr. Steven B. Olsberg ran the indirect tensile tests and the uniaxial compression tests. Mr. Douglas D. Boyer conducted the swell tests and the slake durability tests. Mr. Gregory A. Brekken and Mr. Timothy J. Vogt conducted the point load index tests. Mr. Rodger D. Arnold and Mr. John R. Simonson logged the core and meticulously prepared the samples. Mr. Terry L. Hall drafted the figures, and the report was typed by Ms. Sheree D. Coats and Ms. Alys J. Lafler. This report has been technically reviewed by Dr. Arlo F. Fossum and it was editorially reviewed by Ms. Julie S. Annicchiarico. The cooperation and diligence of these individuals are appreciated.

Francis D. Hansen
Timothy J. Vogt

TABLE OF CONTENTS

TABLE OF CONTENTS
(Continued)

LIST OF TABLES

LIST OF FIGURES

1.0 INTRODUCTION

1.1 BACKGROUND

The experimental work discussed in this report is part of an ongoing program conducted at Oak Ridge National Laboratory (ORNL) concerning evaluation of sedimentary and other rock types as potential hosts for a geologic repository. These evaluations are part of the Repository Technology Program (RTP) that has as objectives the development of tools and techniques for repository characterization and performance assessment in a diversity of geohydrologic settings. This phase of the program is a laboratory study that investigates fundamental thermomechanical properties of several different shales. Laboratory experiments are intrinsically related to numerical modeling and in situ field experiments, which together will be used for performance assessment.

Shales possess the following characteristics that are considered attributes relative to siting a geologic repository: (1) strata in the U.S. are located at appropriate depths and have large vertical and lateral dimensions; (2) they possess a high ion exchange capacity; (3) unfractured shales have a very low permeability; and (4) many shales are relatively plastic, a characteristic that can promote self-healing of fractures and ensure low permeability. Shales do, however, possess characteristics that may prove to be hindrances for potential repository siting, namely: (1) shales can have a low compressive strength; (2) shales may creep readily which could compromise the stability of the underground workings; and (3) thermal effects on the mechanical properties are complicated and not well known.

Thermomechanical data are needed to define parameters used in numerical modeling, as well as for design and operation of a repository. The material properties of greatest interest depend on the rock type under consideration. For example, strength and creep of intact granite are of little concern for a repository in crystalline rock, but these same parameters are essential for characterizing rocks like clays and some shales. The existing literature abounds with mechanical strength measurements of many rock types. Compressive strength, Young's modulus, Poisson's ratio, and angle of internal friction for many sedimentary rocks, including shales, can be gleaned from published documents [Croff et al., 1987]. These data are not sufficient for the needs of the Repository Development Program because in almost every case, basic supporting information such as definitive lithology (mineralogy), depth (of specimen origin), and test conditions is not available in the accompanying literature. Fewer thermal properties such as conductivity, specific heat, and expansion are available in the literature, and they also suffer from a lack of accompanying rock characterization. Therefore, there is

insufficient information on many important thermomechanical properties needed for design, operation, and performance assessment of a repository in a shale medium.

This report addresses strength properties of several diverse shales. Most of the shales were tested in unconfined compression at room temperature and 150°C. Other quantitative and qualitative strength measures include ambient tests of indirect tensile strength, point load index, slake durability, free swell, and swell pressure. Each shale type is generally described and X-ray diffraction is used to identify the mineral composition. Properties of the shales investigated here vary widely; nonetheless, these experiments identify ranges in strength, mineralogy, and durability applicable to some classifications of shale in the U.S.

1.2 APPROACH AND SCOPE

The suite of experiments conducted on shales for this report is given in Table 1-1. These tests were selected as those that could be accomplished without capital investiture or development, could be run on a wide class of rocks, generally did not require large amounts of core, and represent a background of properties useful for comparisons between shales. The tested shales represent a spectrum of material properties encompassing much of the spectrum exhibited by shales. The tested shales include Pierre, Green River, Rhinestreet, Carlile, and others.

This report presents the results of these experiments. Data are presented in many figures and tables throughout the text and in the appendixes. At this point, little comparative analysis is made between the shales tested here. Basically, the ranges in compressive and tensile strength, durability, swell, etc., are presented to show the extreme differences in these properties. A somewhat more detailed examination is made of the Pierre Shale because core from five different members was available.

1.3 REPORT ORGANIZATION

Chapter 2 summarizes the pertinent Quality Assurance documents and procedures used in this study. Chapter 3 describes the shales tested in this investigation and includes the X-ray diffraction data. Chapter 4 contains the bulk of the laboratory data. Chapter 5 summarizes general conclusions and is followed by the list of references. For reading ease, many tables of data and figures are included in appendixes. The contents of the appendixes are as follows: (A) unconfined compression tests on shales: stress-strain curves at room temperature; (B) unconfined compression tests on shales: stress-strain curves at 150°C;

Table 1-1. Experiments on Shales

Experiment Type	Specimen Dimensions (mm)		Temperatures (°C)	Pressures (MPa)
	Diameter	Length		
Quasi-static Compression	50	125	20 and 150	Unconfined
Tensile	50	25	20	NA
Creep	100	200	25 and 100	3.5
Slake Durability	Lumps [50 grams]		20	NA
Free Swell	50	15	20	0.007[a]
Swell Pressure	50	15	20	Variable
Point Load	Variable		20	NA

(a) Soil mechanics convention (0.007 MPa = 1 psi).

(C) indirect tensile strengths of shales; (D) point load indexes of shales; (E) creep tests on Green River specimens; and (F) free swell of shales.

2.0 QUALITY ASSURANCE

Work performed for this report was conducted in accordance with a company-wide Quality Assurance Program [Mutter, 1984]. A number of technical laboratory procedures listed below were used.

Procedure	No.	Rev.	Rev. Date
• Core Acquisition, Shipping, and Storage	TP-01	1	(11/05/82)
• Rock Specimen Preparation	TP-02	1	(11/05/82)
• Jacketing of Solid Cylindrical Specimens for Triaxial Testing	TP-03	1	(11/05/82)
• Direct and Indirect (Brazilian) Tension Experiments	TP-04a	0	(11/05/82)
• Triaxial Compression and Creep Experiments	TP-04b	2	(08/28/86)
• Constant Strain Rate Triaxial Compression Tests	TP-04e	1	(10/08/85)
• Data Acquisition, Reduction, and Storage	TP-05	1	(11/05/82)
• Logging and Preserving Rock Core at the Borehole Site	TP-09	0	(10/08/85)
• Determining the Point Load Strength Index	TP-10	0	(10/17/85)
• Slake Durability Index Test	TP-11	0	(10/08/85)
• Swell Pressure Test	TP-12	0	(10/15/85)
• Swell Potential Test	TP-13	0	(10/15/85)

The technical procedures involve several standard calibrations listed below.

Procedure	No.	Rev.	Rev. Date
• Calibration of Pressure Gauges	CP-01	1	(12/22/80)
• Calibration and Verification of Pressure Measuring Systems	CP-02	2	(12/16/86)
• Calibration and Verification of Load Measuring Systems in Testing Machines	CP-03	3	(12/16/86)
• Calibration and Verification of Deformation Measuring Systems	CP-04	2	(12/16/86)
• Calibration and Verification of Temperature Measuring Systems	CP-08	1	(12/16/86)
• Calibration, Recall, and Filing of Calibration Records	CP-11	0	(11/05/82)

Periodic audits are performed by Quality Assurance to verify compliance with all aspects of the Quality Assurance Program and Quality Assurance Plan. The periodic audits are supplemented by randomly scheduled surveillances of the activities. Nonconformances (findings) identified during these audits and surveillances are documented on a Nonconformance Report (NCR).

Swell pressure, free swell tests, and X-ray diffraction analyses were conducted outside of the RE/SPEC Inc. laboratory. When vendors outside of RE/SPEC are used for technical services, the quality of the product is ensured by either following a procedure in the RE/SPEC Quality Assurance Manual or by showing that the vendor has in place an equivalent Quality Assurance Program. Procedures for free swell and swell pressure tests are included in RE/SPEC's Quality Assurance Manual [Mutter, 1984]. The firm that performed X-ray diffraction operates under a Quality Assurance Program approved and audited by the Environmental Protection Agency (EPA) and the State of South Dakota.

3.0 SHALES INVESTIGATED

3.1 GENERAL DESCRIPTION

Six shales from within the United States were obtained for these evaluations. Four shales were obtained in sufficient size and quantity to conduct compression experiments. These shales are described below. Also noted is the moisture content of each which was determined by drying about 200 g overnight in an oven at 105°C [Lambe, 1951].

1. **Pierre:** The Cretaceous age Pierre Shale cores were from three holes located in Gregory County, South Dakota. The samples were approximately a year old when experiments were run. Between field acquisition and laboratory testing, the cores were reasonably well preserved by being first wrapped in aluminum foil, then completely encapsulated in wax within cardboard tubes. Five members of the Pierre Formation were represented within the core. In general, the material is very fragile and fissile. Original diameter of the core is about 80 mm. It is also plastic and saturated, containing approximately 20 percent water by weight.

2. **Green River:** Samples of the Tertiary age (Eocene) Green River Formation were obtained from the Colony Mine near Parachute, Colorado. Six-inch diameter cores were taken vertically and horizontally from strata within the mine that had a relatively low kerogen content (15 to 20 gallons per ton). These cores were redrilled to suit specific testing requirements. This rock is highly indurated, brittle, and contains less than one percent water by weight.

3. **Rhinestreet:** Rhinestreet Shale from the Devonian age Rhinestreet Formation was obtained from a well in Wirt County near Munday, West Virginia. A total length of approximately 15 m of 85-mm-diameter core was recovered, however, the entire length was broken into short discs parallel to bedding. The discs of this material are hard and relatively brittle and there is little cohesion between discs. The Rhinestreet Shale contains a little over one percent water by weight.

4. **Carlile:** Air-dried core from the Upper Cretaceous age Carlile Formation was obtained from near Igloo, South Dakota. It is a carbonate-rich montmorillonitic shale, however, its in situ water content is not determinable from the available core. The strength properties measured here reflect an increase attributable to the water loss.

Samples of two other shales were also obtained in smaller quantities which were sufficient for limited characterization. About 200 mm of air-dried core was obtained of each of the Cambrian age Conasauga Shale near Oak Ridge, Tennessee, and of the Mississippian/Devonian age Chattanooga Shale near Carthage, Tennessee. X-ray diffraction was used to identify constituent minerals and a few point load index tests were conducted on these shales.

3.2 SPECIMEN IDENTIFICATION

Each specimen is given an identification number. Occasionally, two different experiments are run on parts of the same piece of core (such as the X-ray diffraction and the swell potential tests) and these samples have identical identification numbers. Sample identification always starts with an abbreviation of the source rock (e.g. GR = Green River) separated by a slash (/) from the year of preparation. Subsequent numbers relate to the bore hole if there is more than one hole per site and other details of finishing that depend on the type of test. Specimens that require recoring and finishing have a systematic scheme that is part of a standard Quality Assurance procedure (Laboratory Procedure TP-01, Rev. 2, RE/SPEC Laboratory Procedure Manual). For example:

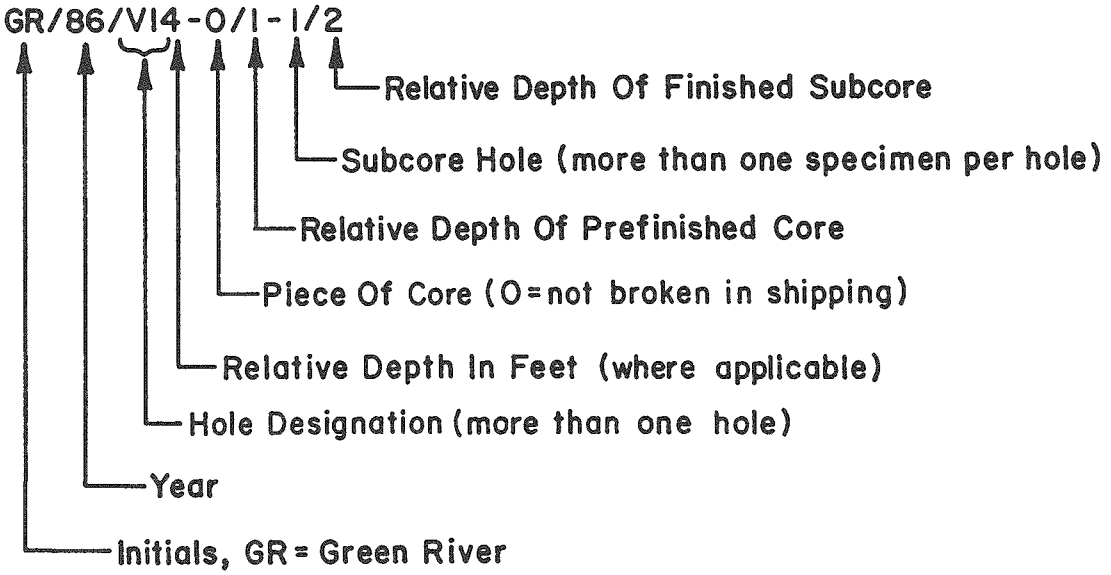

3.3 X-RAY DIFFRACTION

The purpose of X-ray diffraction analyses is to identify the major mineralogical constituents of each rock type. In turn, this allows comparisons to be made between

mineralogical composition and mechanical properties. Generally, it is the lack of petrographic information that precludes from use much of the mechanical data that exists in the literature. The number of tests in this report are often too limited to conclusively relate lithology and mechanical properties, but to make useful comparisons of shale data throughout the literature one needs both mechanical and mineralogical measurements. The Pierre Shale, of which five individual members are available, allows comparisons between composition and swell characteristics for this shale type.

3.3.1 Procedure

The general techniques of mineral identification using X-ray diffraction are well established and many standard references are available for an introduction to this topic. The analyses presented here were completed using the Reference Intensity Method (RIM) of quantitative X-ray diffraction analysis. This method permits quantitative multicomponent analyses of crystalline material without requiring preparation of calibration curves, and more recently, without the need for adding an internal standard to the sample [Davis and Walawender, 1982; Chung, 1974a, 1974b, 1975]. This method requires the attainment of random orientation of crystallites throughout the diffracting volume of the sample. This random orientation has been successfully achieved by loading the particles in the form of an aerosol onto an irregular fibrous filter [Davis, 1984]. In addition to the analysis of crystalline components, the amount of up to two amorphous components can be determined by the use of automated X-ray transmission (AXRT) in combination with regular diffraction analysis.

X-ray diffraction data were obtained from tests on the trimmings of specimens used in swell potential tests. Specimens were selected within each shale group from the material having the highest and lowest swell potential. This selection procedure was predicated on the assumptions that mineralogical composition is an important factor influencing swell potential and that X-ray data could delineate the range in composition within each group.

Each sample was ground to reduce the material to the appropriate size (ideally 10 microns). The powder was then suspended as an aerosol and collected onto a glass fiber filter in a uniform layer. The X-ray analyses were then performed using the randomly oriented sample as collected on the filter. The analyses yield a final weight fraction and variance error for each component, crystalline, and amorphous.

3.3.2 Quality Assurance

Quality Assurance procedures [Davis, 1987] were developed under an Environmental Protection Agency mandate for performance under air quality research projects completed during the past 10 years. Because of the varied aspects of analytical work continuing in the X-ray laboratories, this procedure has been maintained and amplified in all current and proposed projects. Periodic checks and calibrations of several instruments, as well as procedures for reproducing results in reference constants, are made.

The X-ray diffraction (XRD) system is checked for alignment and proper performance on a weekly basis regardless of the particular use. A quartz novaculite standard is scanned and the intensity integrated each week and recorded in a log book. These diffraction standard intensities may be used to adjust actual sample values for minor misalignment or sample height differences from week to week. For reference constant measurements, the XRD analyses are made in duplicate or triplicate to evaluate some degree of precision. Final weight percentages are means of several analyses obtained for different specimens or chemical preparations.

3.3.3 Compositional Data

Shales exhibit extreme variability in composition reflecting the wide range of source materials that make up this fine-grained clastic rock. In particular, vertical heterogeneity can be large. The compositional results presented here represent only a small sample population of this widely variable material. Table 3-1 summarizes the weight percentages of principal mineral groups and amorphous components in the various shales examined in this study.

Four clay mineral groups are represented: illite, chlorite, kaolinite, and smectite. Smectite is synonymous with the montmorillonite group of clay minerals. The total nonclay detrital category is composed of both quartz and feldspar. Dolomite, calcite, and siderite are combined in the total carbonate column. The carbon column includes amorphous carbon matter identified using the AXRT method described above. One sample of the Mobridge member of the Pierre Shale Formation which displays high carbon content was also unique in that it also displayed a distinct "oily" odor. As noted on the table, that particular analysis was not included in the correlations due to its anomalous nature. The "Other" category includes several minerals. Bassanite is the only "other" mineral identified in the Verendrye, Elk Butte 1, and Virgin Creek 2 samples. Gypsum is the only "other" mineral in the Mobridge 2 sample. Gypsum, jarosite, and stilbite occur in the Elk Butte 2 sample, and gypsum occurs with limonite in the Virgin Creek 1 sample. The "other" mineral in the Green River sample is analcite.

Table 3-1. Weight Percentages of Minerals in Shales

Shale Sample I.D.	Mineral Type								
	Illite	Chlorite	Kaolinite	Smectite	Nonclay Detrital[a]	Total Carbonate[b]	Organic Carbon	Pyrite	Other
Verendrye[c] PS/86/20U21/453	27.3 ± 3.8[d]	0.0	2.1 ± 0.5	32.6 ± 4.1	34.9	1.7	0.0	0.7 ±.09	0.6
Elk Butte 1[c] PS/86/20U4/106	14.3 ± 2.1	0.0	7.7 ± 2.0	26.3 ± 4.4	32.6	16.8	0.0	0.7 ±.11	1.5
Elk Butte 2[c] PS/86/19U7/172	10.9 ± 1.4	0.0	4.1 ± 1.1	31.7 ± 4.3	36.4	10.3	0.0	0.9 ±.11	5.7
Mobridge 1[c] PS/86/20U13/295	13.6 ± 2.1	0.0	8.7 ± 2.3	25.1 ± 4.4	32.9	19.1	0.0	0.6 ±.09	0.0
Mobridge 2[c] PS/86/20U8/193	3.5 ± 1.4	2.3 ± 0.1	1.9 ± 0.1	13.1 ± 5.5	14.6	56.5	4.6[e]	1.1 ±.42	2.5
DeGrey[c] PS/86/20U23/493	5.5 ± 1.0	1.5 ± 0.3	0.0	31.2 ± 8.6	54.7	0.0	0.0	1.1 ±.21	6.2
Virgin Creek 1[c] PS/86/20U17/374	34.5 ± 3.5	0.0	0.7 ± 0.2	41.1 ± 4.6	22.4	0.3	0.0	1.0 ±.13	0.0
Virgin Creek 2[c] PS/86/20U17/374	12.0 ± 1.5	0.0	1.5 ± 0.4	41.7 ± 4.6	42.1	0.5	0.0	1.1 ±.13	1.2
Carlile IG/86/C10D-0/2-1/1	9.3 ± 1.1	0.0	11.0 ± 2.7	19.2 ± 3.0	55.4	4.3	0.0	0.8 ± .10	0.0
Conasauga Not assigned[f]	53.4 ± 3.4	20.4 ± 3.0	0.0	0.0	24.0	0.0	0.0	2.2 ±.25	0.0
Chattanooga Not assigned[f]	20.8 ± 2.2	0.0	1.4 ± 0.4	20.3 ± 3.1	50.9	0.0	0.0	6.5 ±.70	0.0
Green River GR/86/V34-0	3.9 ± 0.6	0.0	0.0	0.0	31.3	50.5	6.0	0.0	8.3
Rhinestreet DR/86/160	31.0 ± 3.8	20.1 ± 3.3	0.0	0.0	20.6	25.4	2.4	0.4 ±.07	0.0

(a) Total nonclay detritals consist of quartz and plagioclase feldspars.
(b) Total carbonates consist of calcite, dolomite, and siderite.
(c) Individual members of Pierre Formation.
(d) ± indicate standard deviation, only on monomineralic categories.
(e) This analysis was not used for correlations due to its high organic content.
(f) Inadequate material for individual sample identification.

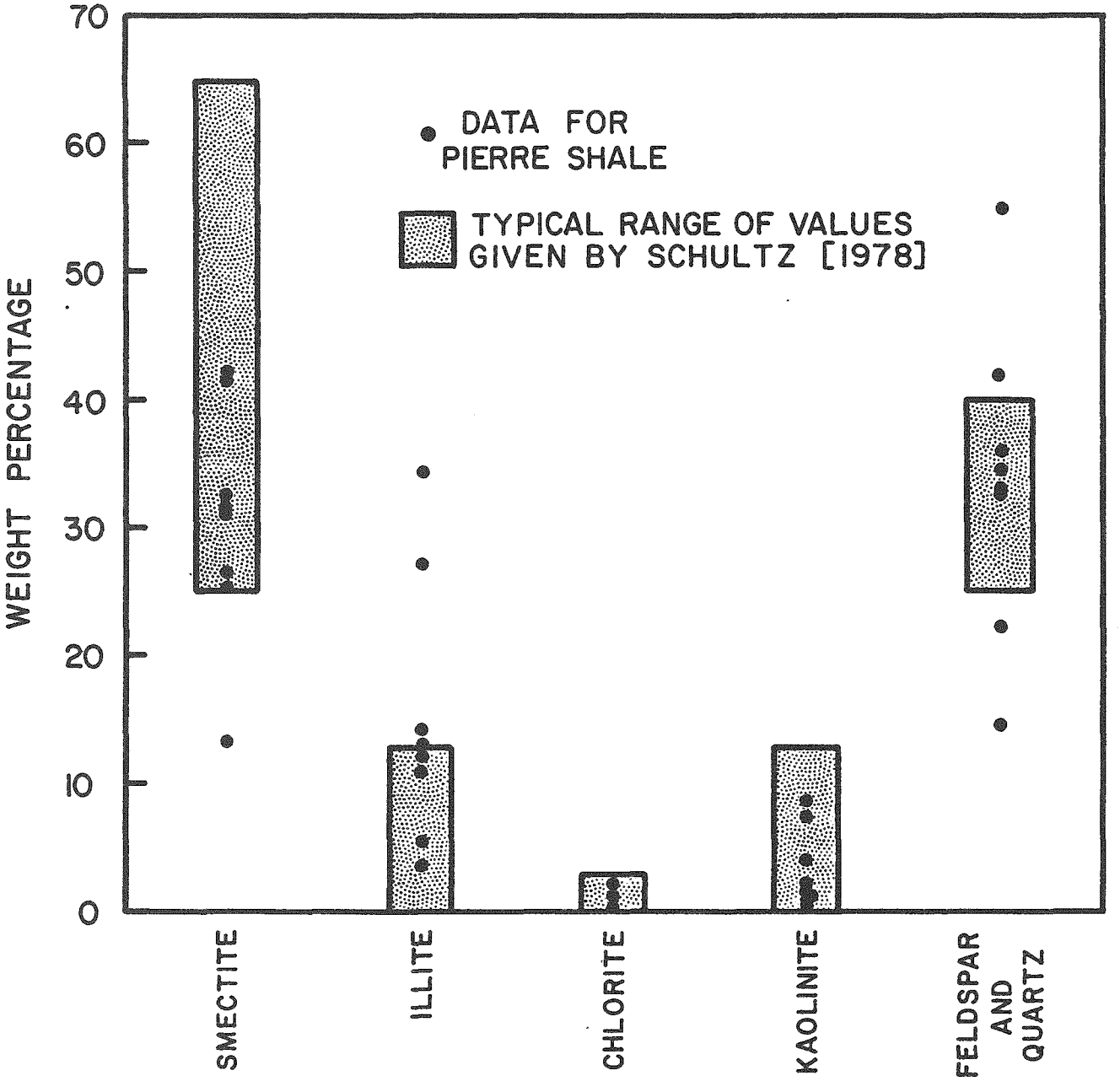

Figure 3-1. Mineralogical Composition in Weight Percent for Pierre Shale

The X-ray diffraction data can be used to compare the mineralogy of shales tested for this report with the broad ranges of other possible shales. Note that a total of eight analyses were run on the Pierre Shale, primarily because several members of the formation were available. On average, the Pierre Shale has about 50 percent clay minerals, mostly smectite. The Pierre Shale also contains an average of 36 percent quartz and feldspars detritals, and is considered a representative smectitic shale. Figure 3-1 compares the composition of the Pierre Shale tested in this study to the typical range for Pierre Shale as determined by Schultz [1978].

Only one X-ray analysis was run for each of the other shale types. These shales exhibited minimal amounts of swelling, developed almost no swell pressures, and are in general less variable mineralogically. Only one X-ray analysis is probably insufficient for future comparisons between mineralogy and mechanical results because of the variability within individual members. As an example, the analyses of two samples of the same member of the Pierre Shale illustrate that a general classification might be justifiable (such as "a shale that contains large amounts of smectite"); but in detail, the percentages of each mineral type are quite variable. Mindful of this caveat, the Conasauga and Rhinestreet Shales are generally classified as "illitic," inasmuch as they consist of over 50 percent nonswelling clays, of which most is illite. The Chattanooga Shale contains 20 percent illite (nonswelling) and 20 percent smectite (swelling). The Green River material contains a minimal amount (3.9 percent) of clay minerals, over 50 percent carbonates, especially dolomite, and 31 percent quartz and feldspars. The Green River material is therefore not a shale at all. It has been called a marl, which typically is 65 to 35 percent carbonate and 35 to 65 percent clay minerals [Pettijohn, 1975]. The Green River Formation is often discussed generally as a shale and because this misnomer pervades the literature, tests were conducted here to compare this rock with other shales. Furthermore, in the text it will be convenient to summarize the data in synoptic tables and figures that will often be entitled generally as "shale," although it is recognized that the Green River material falls outside the classification of shale.

4.0 RESULTS

4.1 UNCONFINED COMPRESSION

4.1.1 Ambient Tests

The unconfined compressive strength, Young's modulus and Poisson's ratio at room temperature, were measured on three specimens each of Carlile, Green River, and Rhinestreet cores and four specimens of Pierre Shale. Specimen deformation was measured by transducers mounted on the specimen. The axial deformation transducer has two arms that measure deformation over a 50-mm-gage length on opposite ends of a diameter. Transducer output is equal to the average output of the arms. The circumferential transducer measures average radial displacement at specimen midheight. This transducer comprises a roller-link chain that encircles the specimen and a sensor that responds to relative motion of the ends of the chain. Testing machines are all calibrated against traceable load and displacement standards. All experiments followed approved laboratory procedures documented in RE/SPEC's Laboratory Procedures Manual.

Stress-strain response of these materials is far from ideally elastic, and therefore some subjective consideration is given to calculation of elastic modulus, E, and Poisson's ratio, ν. Most of the deviation from linear response occurs in the measurement of axial displacement. An accentuated displacement, resulting in an apparent large strain, occurs early in the loading history and is attributed to closure of horizontal laminae. After a load of about 1 MPa, the axial displacement becomes nearly linear. Calculations of E and ν are made from the linear portions of the stress-strain curves at a stress of approximately one half of the ultimate strength.

A summary of strengths, elastic moduli, and Poisson's ratios is given in Table 4-1, and plots of lateral and axial strains versus axial stress are given for individual tests in Appendix A. Strengths range from an average of 7.2 MPa for the soft, wet Pierre Shale to 94.8 MPa for the calcareous Green River material. The Carlile Shale averages 22.8 MPa in the dry condition, no doubt exhibiting a greater strength because of moisture loss. The Rhinestreet Shale, although fissile, is very strong (58.7 MPa) when loaded perpendicular to bedding.

In general, elastic modulus increases with increasing compressive strength. Calculation of E is made over the most linear portion of the stress-strain curve. The nonlinearity of response must also be taken into account when calculating ν. Because Poisson's ratio is the lateral strain divided by the axial strain, excessive axial displacement diminishes the calculated value of ν. The initial, nonlinear axial

Table 4-1. Mechanical Data For Unconfined Compression Tests at Room Temperature

Shale Type	Sample I.D.	Ultimate Strength (MPa)	Young's Modulus, E (GPa)	Poisson's Ratio, ν
Pierre	PS/86/20U8-2/1-1/1	7.6	0.6	0.10
	PS/86/20U8-4/1-1/1	7.0	0.6	0.13
	PS/86/20U11-2/2-1/2	7.4	0.6	0.15
	PS/86/20U8-4/2-1/1	6.9[a]	0.6	0.11
Average ± Standard Deviation		7.2 ± 0.3	0.6 ± 0.0	0.12 ± 0.02
Rhinestreet	DR/86/129/1-1/1	58.9	16.0	0.18
	DR/86/115/1-1/1	60.3	20.6	0.20
	DR/86/251/1-1/1	56.9	15.8	0.19
Average ± Standard Deviation		58.7 ± 1.7	17.5 ± 2.7	0.19 ± 0.01
Green River	GR/86/V14-0/1-1/1	84.6	10.3	0.30
	GR/86/V34-02-3/1	108.2	12.7	0.30
	GR/86/V26-0/1-2/1	91.7	8.2	0.32
Average ± Standard Deviation		94.8 ± 12.1	10.4 ± 2.3	0.31 ± 0.01
Carlile	IG/86/C10B-0/1-1/4	20.4	1.2	0.10
	IG/86/C10D-0/2-1/1	26.4	3.5	0.21
	IG/86/4B-0/1-1/2	21.7	5.2	0.17
Average ± Standard Deviation		22.8 ± 3.2	3.3 ± 2.0	0.16 ± 0.06

(a) Broken along bedding plane before testing.

displacement is subtracted before these calculations are made. Even so, the Poisson's ratios of the materials are relatively low, ranging from 0.10 to 0.32.

The values of unconfined compressive strength and Young's modulus of Pierre Shale can be compared to results reported by Abel and Gentry [1975]. The mechanical results of Abel and Gentry are not accompanied by petrographic descriptions or X-ray mineralogy, therefore, we can only establish that our results fall within a rather broad range. As given in Table 4-1, the Pierre Shale averages 7.2 MPa and 0.6 GPa for unconfined compressive strength and modulus of elasticity, respectively. These values compare favorably with the ranges reported by Abel and Gentry of 0.5 to 17.5 MPa for unconfined compressive strength and about 0.2 GPa for the modulus. In the absence of specific member identification, mineralogy and perhaps calculational techniques, it is difficult to compare further these data for Pierre Shale.

Mechanical Properties of Green River Formation have been widely published [e.g., Costin, 1980], which provides an opportunity to compare the strength and elastic properties determined here with those reported by others. At room temperature, elastic properties of oil shale correlate well with the kerogen content. The kerogen content of our samples is about 15 to 20 gpt. On average, this grade of oil shale has an elastic modulus of about 12 GPa and a Poisson's ratio of 0.25 to 0.30. In addition, Green River material of similar kerogen content has an unconfined compressive strength of about 100 MPa. These published values are in agreement with results found here.

The average unconfined compressive strength of the Rhinestreet Shale falls about midway of the range of values reported for other Devonian shales from the Applachian Basin [Blanton et al., 1981]. Typical unconfined strengths of Devonian shales average 87 MPa and 69 MPa for black and grey shales, respectively. Our samples of Rhinestreet average 59 MPa. The Young's modulus of Rhinestreet is also less than the average of the grey and black Devonian shales (17.5 GPa versus 30 GPa). Again, to be meaningful, comparisons of shale data require mineralogical data and other supporting information.

Similar comparisons cannot be made accurately with the other shale data because of inadequate published descriptions of lithologies. The strengths and elastic moduli listed in Table 4-1 are tenable, but overall the Poisson's ratios are relatively low, as anticipated values for soft rocks are usually around 0.4. It is possible that the Poisson's ratios of some of the shales are apparently low because the axial deformation measurement includes a pressure-dependent closure of cracks along sedimentary layering that is not apparent from the stress-strain curves.

4.1.2 Tests at 150°C

Samples of the Green River and Rhinestreet Formations were tested in unconfined compression at 150°C. The other shales were not tested under these conditions because a sufficient amount of core was not available. The test technique was very similar to the ambient tests, although a different test apparatus was used. Tests at 150°C required the use of a viton jacket because the specimens were surrounded by oil. Once again, these procedures are described fully in the RE/SPEC Laboratory Procedures Manual. A summary of the mechanical results is given in Table 4-2, and the stress-strain plots are given in Appendix B.

Table 4-2. Mechanical Data For Unconfined Compression Tests at 150°C

Shale Type	Sample I.D.	Ultimate Strength (MPa)	Young's Modulus, E (GPa)	Poisson's Ratio, ν
Rhinestreet	DR/86/116/1-1/3	73	26.0	0.14
	DR/86/258/2-1/1	70	13.8	0.12
	DR/86/243/1-2/1	81	15.2	0.10
Average ± Standard Deviation		74.7 ± 5.7	18.4 ± 6.7	0.12 ± 0.02
Green River	GR/86/V14-0/1-2/1	22	0.8	(a)
	GR/86/V34-0/2-2/1	27	1.1	(a)
	GR/86/V26-0/1-3/1	25	0.5	(a)
Average ± Standard Deviation		24.7 ± 2.5	0.8 ± 0.3	(a)

(a) Jacket expanded, see text.

The effects of temperature on the strength and deformational characteristics of Rhinestreet Shale are not too severe. Generally, the material became stronger and more brittle at 150°C. Note an increase in strength to 74.7 MPa compared to 58.7 MPa at room temperature. Young's modulus increased slightly to 18.4 GPa while Poisson's ratio decreased to 0.12. These modest changes can be attributed

to drying of the sample, and because the material contained only a little over one weight percent water, the effects are minimal.

A temperature of 150°C has dramatic effects on the mechanical properties of Green River Shale, as expected [e.g., Chong and Smith, 1984]. Strength is reduced from an average of 94.8 MPa at room temperature to 24.7 MPa at 150°C. Young's modulus is reduced by more than an order of magnitude. Reduction in strength and an attendant increase in deformability with elevated temperature are attributed to softening and more plastic deformation of the organic content. At ambient conditions the kerogen is stiff; however, at elevated temperature its viscosity is reduced and gases are formed. Expansion of the gaseous volatiles ballooned out the viton jacket and the circumferential transducer as well. The result is an erroneously large apparent lateral strain.

4.2 INDIRECT TENSION

Indirect tensile strength was determined by means of the Brazilian test (TP-04a, RE/SPEC Laboratory Procedures Manual). This is an indirect method in which a diametral line load is applied over the length of a rock cylinder (parallel to bedding) having a length-to-diameter ratio L:D $\cong$ 0.5. The apparent tensile strength is computed by:

$$T_o = 2P/\pi DL$$

where

T_o = tensile strength
P = the line load required to initiate fracture along the diameter
D = the specimen diameter
L = the specimen length.

The failure load is defined to be the peak load before the first drop in load. Indirect tensile specimens were loaded parallel to bedding. Both curved and flat platens were used in this study in an attempt to quantify differences that may be attributable to test technique. On average, no consistent differences were noted in the strengths resulting from the different platens. If a systematic difference exists between the results from curved and flat platens, it is less than the natural variability of the tested material. Appendix C lists the indirect tensile strengths of all the tests and each shale type is discussed below.

4.2.1 Pierre Shale

Seventeen specimens were successfully tested. Tests were made on 38-mm-diameter specimens that were trimmed on a lathe to remove circumferential ridges.

All tests were made using flat platens. The tensile strength of Pierre Shale ranges from 0.31 to 0.83 MPa and averages 0.53 ± 0.13 MPa (about 75 psi). The standard deviation is relatively small indicating consistency in the data.

4.2.2 Green River Formation

Twenty-two specimens of 50-mm-diameter Green River Core were tested. The average tensile strength is 11.9 ± 2.4 MPa (1,725 ± 350 psi), and the range is from 6.8 to 16.3 MPa. Eleven tests using curved platens average 13.2 MPa, and 11 using flat platens average 10.6 MPa.

4.2.3 Rhinestreet Shale

Eighteen specimens of 50-mm-diameter Rhinestreet Shale were tested, and one test was aborted. Strength ranges from 5.1 to 12.2 MPa and averages 8.4 ± 1.9 MPa (1,220 ± 275 psi). Curved platens yield 7.5 MPa, while flat platens average 8.4 MPa.

4.2.4 Carlile Shale

A total of 18 tests were conducted on 50-mm-diameter specimens of Carlile Shale. Tensile strength ranges from 2.1 to 8.8 MPa and averages 3.5 ± 1.5 MPa (500 ± 200 psi) for all tests. Nine specimens were tested using flat platens and nine using curved platens. On average, the strengths for each group differed by only 5 percent; thus, no effect of the platens is observed.

4.3 POINT LOAD INDEXES

The point load test is an index test for strength classification of rock materials. It may be used as a measure to predict other strength parameters with which it is correlated, such as tensile or unconfined compressive strength. The particular value of this strength index is that the test can be performed on specimens with little or no special preparation. Basically, the test arrangement subjects a specimen to a load applied by spherically truncated, conical platens. A valid failure requires the fracture to pass through each of the platen contact points. Softer rocks such as the Pierre, Carlile, and Chattanooga often allow deep penetration of the conical platens which in turn results in a large percentage of invalid failures. The resulting failures are localized at each individual platen rather than bisecting the sample. In contrast, the relatively harder Green River Formation almost always failed in a valid manner. The procedures involved in determining the point load strength

index follow TP-10, RE/SPEC Laboratory Procedures Manual. The point load test is becoming an acceptable and recognized test, and a "standard" suggested method has been developed by the International Society for Rock Mechanics Commission on Testing Methods [ISRM, 1985].

As noted, one of the attractive features of the point load test is its use on a variety of specimen sizes and shapes. This is particularly useful for characterizing fissile rocks where few cores are available for more conventional experiments. In consideration of the various specimen sizes, a standard size correction is often used so the results can be discussed in terms of a standard value. The standard size is 50 mm (approximately 2-inch diameter), and the point load indexes are reported here as $I_s(50)$ values. Samples of other sizes are corrected to the $I_s(50)$ value according to calibrated correction charts.

Suites of ten or more point load tests were conducted on Pierre, Green River, and Carlile cores. A few small specimens of the Chattanooga Shale were also tested. An attempt was made to test the Rhinestreet Shale, but incompetence of the bedding planes prevented successful testing. The available specimens of Conasauga Shale proved to be too small to test. The results and observations for each of the shales are discussed separately below.

4.3.1 Pierre Shale

The specimens used for the point load testing of the Pierre Shale consisted of various lengths of core which ranged from 50 to 75 mm in diameter. Each piece of core having sufficient dimensions for diametral testing (parallel to bedding) was used for that purpose. Shorter pieces and often pieces resulting from the diametral test were used for axial tests (perpendicular to bedding).

Only five of eighteen diametral tests were valid; seventeen of twenty-one tests in the axial orientation were valid. Most fractures resulting from diametral tests were bedding-plane controlled. However, the bedding planes themselves commonly underwent deformation that invalidated the test. The specimens were so soft that the platen cones would often penetrate the specimen deeply before initiating fracture. This created a series of apparent loading and unloading cycles caused by the penetration-fracture-penetration sequence. These problems were not encountered in the axial orientation. Table D-1 in Appendix D gives the results of the successful tests. The average index strength perpendicular to bedding is 0.27 MPa and 0.13 MPa parallel to bedding giving the index of anisotropy of 2.

4.3.2 Green River Formation

The specimens used for the point load testing of the Green River material consisted of core approximately 50 mm in diameter and 125 mm long. Each length of core was initially tested in a diametral orientation, parallel to bedding, near the center of its length. Each of the two resulting pieces was also tested in the diametral orientation near its center. The four shorter pieces of core were then tested in an axial orientation, perpendicular to bedding.

In total, 12 diametral tests were attempted and all specimens failed in a valid mode; i.e., the fracture passed through the platen contact points. Sixteen axial tests were attempted but only 14 failed in a valid mode. Table D-2 in Appendix D gives the results of the successful tests. The average index strength perpendicular to bedding is 4.02 MPa. The average strength parallel to bedding is 2.45 MPa. The index of anisotropy is 1.6. The strength parallel to bedding is, in general, less than that normal to bedding, and not all of the fractures in the diametral orientation were controlled by bedding planes. The failures not controlled by bedding planes showed no other obvious controlling mechanism.

4.3.3 Carlile Shale

The Carlile Shale used for point load tests was approximately 80 mm in diameter and of variable length. The core was air dry. Eighteen diametral tests were attempted with nine giving valid failures. Eleven of fourteen axial tests were successful. Table D-3 in Appendix D gives the results of the successful tests. The average index strength parallel to bedding is 0.51 MPa, and the average strength perpendicular to bedding is 0.91 MPa. The index of anisotropy is 1.8. Diametral breaks were dominantly bedding-plane controlled.

4.3.4 Chattanooga Shale

Only four small pieces of Chattanooga Shale core were available for testing. These pieces were slightly less than 38 mm in diameter and represented less than 200 mm of core. The core was not sealed and is considered air dry. Only two of six diametral tests and two of four axial tests yielded valid failures. Table D-4 in Appendix D summarizes the results. The average index strength parallel to bedding is 0.32 MPa, and the average strength perpendicular to bedding is 3.37 MPa. The resulting index of anisotropy is 10.5.

4.3.5 Rhinestreet Shale

No successful tests were completed on the Rhinestreet Shale, although ten tests were attempted. No specimens were long enough to allow diametral testing, and the bedding-plane weakness was so acute that no valid failures were achieved in the axial orientation. The reason that no tests were valid is that penetration by the cones in the axial tests was sufficient to break the shale along bedding perpendicular to the loading direction.

4.3.6 Summary of Point Load Index Test Results

For most of the shales (the notable exception is the Green River Shale), bedding plane weaknesses controlled strength in orientations parallel to bedding. In every case, the strength of the shales parallel to bedding is significantly less than that normal to bedding. The Green River material is the strongest of the rocks tested in both the diametral and axial orientations, and the Pierre Shale is the weakest.

Comparisons can be made between our results and those published in the literature. Proponents of the point load tests have shown that a straight-line correlation exists ($r = 0.88$) between uniaxial compressive strength and point load strengths [e.g., Broch and Franklin, 1972]. We find the point load index, $I_s(50)$, to be correlated to both unconfined compressive strength and indirect tensile strength. Table 4-3 lists the point load index, the indirect tensile strength, the uniaxial compressive strength, and the ratio of the unconfined strength to $I_s(50)$. Using only the data from these three shale types, correlation is strong between the three mechanical properties. Values of the ratio of unconfined compressive strength, σ_o, divided by $I_s(50)$ range from 23.6 to 26.7, which compares most favorably with a value of 23.7 for many diverse rocks reported in the literature [Broch and Franklin, 1972].

4.4 CREEP

Only the Green River material was tested in the creep mode because it was the only source from which specimens of the appropriate size (100 × 200 mm) could be made. Table 4-4 summarizes the stress and temperature conditions for the multistage tests, as well as the axial strain and total time. This rock is extremely creep resistant even under conditions (axial stress = 31 MPa, temperature = 100°C) that might be considered high for a repository containing heat-generative nuclear waste. Stress-strain curves for each multistage test are given in Appendix E. It is interesting to note that 100°C does not significantly enhance the creep rate as might have been expected based on the dramatic weakening of the unconfined compression tests caused by 150°C. According to DuBow [1984], the observed variation in mechanical

properties of oil shale with temperature arises from the presence of kerogen and its transformation during heating. The loss of light and volatile compounds occurs between 100°C and 150°C, but for this lean grade (15–20 gpt) the volatiles are relatively unaffected by heating to 100°C.

Table 4-3. Point Load Indexes, Tensile, and Compressive Strengths

Shale Type	Point Load Index, $I_s(50)$ (MPa)	Indirect Tension (MPa)	Unconfined Compressive Strength, σ_o (MPa)	$\frac{\sigma_o}{I_s(50)}$
Green River	4.02	11.9	94.8	23.6
Pierre	0.27	0.5	7.2	26.7
Carlile	0.91	3.5	22.8	25.1

Table 4-4. Creep Tests on Green River Specimens

Specimen Identification	Stage	$\Delta\sigma$ (MPa)	$\sigma_2 = \sigma_3$ (MPa)	T (°C)	Total Time (sec $\times 10^6$)	Axial Strain
GR/86/V27-0/1-1/1	1	20.7	3.5	25	2.0	0.0003
	2	20.7	3.5	100	4.8	0.0038
	3	31.0	3.5	100	13.7	0.0052
GR/86/V54-0/1-1/1	1	20.7	0	25	1.5	0.0006
	2	31.0	0	25	15.7	0.0017

The two tests made use of several different stages to assess: (1) the effects of modest confining pressure (3.5 MPa) relative to unconfined, (2) the effects of 100°C temperature relative to ambient, and (3) the effects of differential axial stress ($\Delta\sigma$) changes. The first stage of each test was conducted at $\Delta\sigma = 20.7$ MPa; one specimen was confined at 3.5 MPa and the other was unconfined. Over 23 days (2×10^6 seconds), each specimen deformed minimally. The unconfined specimen sustained an axial strain of 0.0006, and the confined specimen sustained only 0.0003. The

effects of elevating the temperature to 100°C can be seen on Figure E-1, Appendix E. After a transient of about 0.2 percent axial strain, the creep rate began to decrease rapidly. After 35 days, the axial creep rate had decreased to $3(10^{-10})s^{-1}$. In fact, all of the creep rates experienced by the specimens were very low. The last stage of each test was conducted at $\Delta\sigma = 31$ MPa for a duration of about 100 days. The test at 100°C (Figure E-1) achieved a creep rate of $1.8(10^{-10})s^{-1}$, and the test at 25°C achieved at a rate of $1.7(10^{-11})s^{-1}$.

4.5 SLAKE DURABILITY

Slake durability tests are used to measure qualitatively the deterioration of rock due to climatic wetting and drying. The slake durability is a measure of the cohesion of a rock and has been found to be a function of permeability, porosity, and pore fluid [Franklin and Chandra, 1972]. The test procedure (TP-11, RE/SPEC Laboratory Manual) as adapted from the International Society for Rock Mechanics [Brown, 1981] was followed for these tests on shales. The slaking fluid was ordinary tap water at room temperature. The slake durability index is a percentage obtained by dividing the dry weight of the specimen after two cycles of wetting and drying by the initial dry weight of the specimen.

Specimens of Green River, Rhinestreet, and Pierre were tested. The Green River and Rhinestreet specimens were very durable and required only three tests each to yield consistent results. Specimens of Green River Shale and Rhinestreet Shale had to be broken from the core with a rock hammer. The edges and corners were rounded as much as possible to form ten rounded pieces weighing 45 to 55 g each. Specimens of the Pierre Shale were prepared from an approximately 80-mm-diameter core and cut by hand to form ten spherical lumps weighing 45 to 55 g each. Lumps of material for slake durability tests were not given specimen identification numbers.

Slake durability test results are given in Table 4-5. Testing was terminated when it was felt results bracketed inherent variability of each shale. A total of 19 tests were run on the five members of Pierre Shale. Slake durability of each member does not vary appreciably, averaging a little more than 50 percent of the material remaining after two cycles. The Green River and the Rhinestreet material are both very durable and lost almost no weight after two cycles of wetting and drying.

The five members of the Pierre Shale were tested individually to ascertain potential relationships between durability and mineralogy. The Pierre Shale members have similar history, moisture, and lithification. Strong correlations between durability and clay mineralogy are not evident when regression analyses are completed using all the available data. A modest correlation (0.63) is found between the

amount of quartz plus feldspars and durability. This relationship shows that the members with greater amounts of quartz and feldspar are more durable. When trends are visually examined using average mineralogies for each member, they indicate that durability decreases with increasing clay content, particularly illite.

Table 4-5. Slake Durability Test Results

Shale Group	Average[b] (%)	Range (%)	Number of Tests	Classification [Gamble, 1971]
Elk Butte[a]	62.9	41.6 to 79.3	3	Medium
Mobridge[a]	57.7	39.6 to 70.0	4	Low
Virgin Creek[a]	44.1	21.3 to 57.3	5	Low
Verendrye[a]	61.3	51.3 to 65.8	4	Medium
DeGrey[a]	70.6	68.0 to 73.4	3	Medium
Pierre Average	57.8	21.3 to 79.3	19	Low-Medium
Green River	99.8	99.8 to 99.8[c]	3	Extremely High
Rhinestreet	98.0	97.2 to 99.0	3	Extremely High

(*a*) These shales are individual members that comprise the Pierre Shale.
(*b*) Material remaining after two cycles of wetting and drying.
(*c*) All test results are identical.

The results of these tests indicate that embankments, tunnels, or open cuts in the Pierre Shale should have a low resistance to weathering; whereas, similar structures in the Green River Formation or Rhinestreet Shale would be much less affected by weathering.

4.6 SWELL TESTS

Two different swell tests were performed on three shale types. The first, the swell pressure test, measures the pressure that an axially and laterally confined soil or rock exerts when exposed to free water. The second, the swell potential test, is a measure of the volumetric change of a soil or rock in the presence of free water. In the swell potential test, the specimen is free to deform in the axial

direction. The specimens of the Pierre Shale for these tests were trimmed by hand to approximately 50 mm in diameter. Specimens of the Green River Formation and Rhinestreet Shale were cored with a vertical milling machine. Note that traditional soil mechanics experiments are reported using English units so the test results will include the English units with SI equivalents, as necessary.

4.6.1 Swell Pressure

The procedures involved in determining swell pressure are described in the RE/SPEC Laboratory Procedures Manual (TP-12). Swell pressure was measured with a volume change meter (Soiltest Model C-260). A 50-mm-diameter specimen is placed in a lateral confining ring and a piston attached to a proving ring is lowered to the top of the specimen. The proving ring is secured in place and the specimen is exposed to distilled water at 20°C. Deflection of the proving ring and time from the start of the test are recorded. The test is run until the change in deformation is less than 0.0001 inches (0.0025 mm) within a 24-hour period. The maximum deflection of the specimen, and hence the proving ring at the end of the test, is converted into a force which is divided by the specimen area to yield the maximum swell pressure.

Test results are summarized in Table 4-6. Neither the Green River nor the Rhinestreet specimens developed measurable swelling pressure. The Pierre Shale members developed significant swell pressures, as expected of shales containing smectite. Relationships between the swell pressure of each test and physical and mineralogical measurements were analyzed to determine which imparted the strongest influence on the swell pressure. Of three physical properties (initial moisture content, change in moisture content, and initial dry density), mineralogical components (listed in Table 2-1), and the percent total clays, only percent smectite was found to give a positive correlation with swell pressure. Figure 4-1 shows the plot of percent smectite versus swell pressure. The correlation coefficient for the five members of the Pierre Shale is 0.88. All other factors investigated yielded little or no statistically significant correlation with swell pressure.

4.6.2 Swell Potential

The procedures involved in determining swell potential are described in the RE/SPEC Laboratory Procedures Manual (TP-13). The swell potential is determined using a conventional lever-arm apparatus. A 50-mm (2-inch) diameter specimen about 15 mm in length is placed in a consolidation ring, and the ring is placed in a consolidation apparatus. A 1 psi (0.007 MPa) load is applied to the specimen which is then saturated with distilled water at room temperature. The deflection and time are recorded until the specimen deflection over a 24-hour period

Table 4-6. Swell Pressure Tests

Shale Group	Specimen I.D.	Initial Moisture Content (%)	Final Moisture Content (%)	Initial Dry Density (lbs/ft^3)	Final Dry Density (lbs/ft^3)	Swell Pressure (lbf/ft^2)
DeGrey 1	PS/86/20U23/493	17.0	20.2	109.0	108.5	5,380
DeGrey 2		19.7	23.3	105.8	105.3	4,713
Average		18.4	21.8	107.4	106.9	5,047
Verendrye 1	PS/86/20U21/453	12.4	22.3	111.1	110.7	4,662
Verendrye 2		17.9	23.7	108.4	108.1	4,010
Average		15.2	23.0	109.8	109.4	4,336
Virgin Creek 1	PS/86/20U17/374	21.7	26.6	99.8	99.4	4,565
Virgin Creek 2		22.3	27.9	101.6	100.8	8,790
Average		22.0	27.3	100.7	100.1	6,678
Mobridge 1	PS/86/20U13/295	20.8	23.1	103.7	103.3	3,613
Mobridge 2		20.3	23.2	104.5	104.1	4,273
Average		20.6	23.2	104.1	103.7	3,943
Elk Butte 1	PS/86/20U4/106			101.1	100.8	3,256
Elk Butte 2		21.6	21.0	100.2	100.0	1,830
Average		21.6	21.0	100.7	100.4	2,543
Green River 1	GR/86/V34-0	0.5	0.6	134.5	134.5	(a)
Green River 2		0.5	0.5	132.6	132.6	(a)
Average		0.5	0.6	133.6	133.6	(a)
Rhinestreet 1	DR/86/160	1.6	1.7	164.9	164.9	(a)
Rhinestreet 2		1.4	1.6	166.2	166.2	(a)
Average		1.5	1.7	165.6	165.6	(a)

(a) Although it is evident that the slight increase in moisture content would give rise to a finite swelling of the materials, the swell pressure was below resolution.

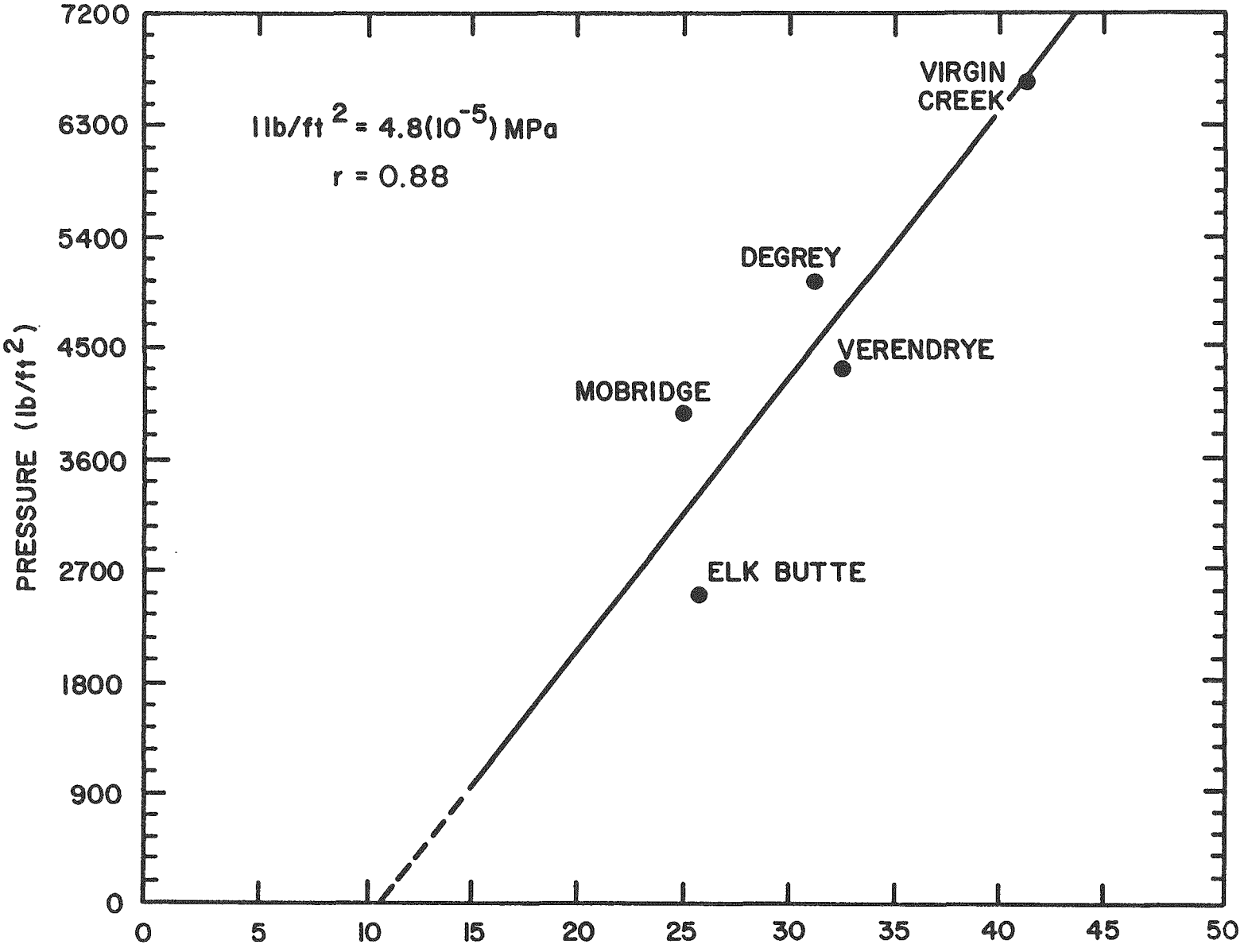

RSI-087-86-23

Figure 4-1. Swell Pressures of Selected Shales as a Function of Smectite Content

becomes less than 0.0001 inches (0.0025 mm). The maximum deflection at the end of the test is divided by the original specimen height to calculate the swell potential.

The results are tabulated in Table 4-7 and plots of deflection over time for tests of each shale type are given in Appendix F. The swell potential (free swell) results are consistent with swell pressure data given previously. The Green River material does not swell at all, and the Rhinestreet swells less than 0.5 percent. Members of the Pierre Shale swell appreciably more and hence are afforded more tests.

The physical and mineralogical properties were correlated with swell potential. The same physical and mineralogical properties were used here as were used in the correlations with swell pressure (i.e., percent illite, kaolinite, smectite, nonclay detritals, calcite, pyrite, initial moisture content, change in moisture, total clay content, and initial dry density). In addition, the average swell pressure test results for each group were correlated with swell potential results.

A moderate correlation exists (correlation coefficient of 0.75) between percent smectite and swell potential, but only a 0.50 correlation between percent total clays and swell potential. This second relationship was unexpected since total clay content had a moderate correlation with swell pressure. A fair positive correlation (0.73) was found between swell pressure and swell potential. This important consistency has been reported previously [Petry and Armstrong, 1980]. Although data here are sparse, swell potential of each individual test of the five Pierre Shale members shows no significant correlations with physical and mineralogical properties except smectite. This may indicate an interplay of a number of variables influencing swell potential that is not obvious within this limited population.

Table 4-7. Swell Potential Tests

Shale Group	Specimen I.D.	Initial Moisture Content (%)	Final Moisture Content (%)	Initial Dry Density (lbs/ft^3)	Final Dry Density (lbs/ft^3)	Swell Potential (% Swell)
DeGrey 1	PS/86/20U23/493	19.3	24.6	106.7	104.1	3.1
DeGrey 2	"	18.3	26.4	107.7	104.5	3.0
DeGrey 3	"	21.1	27.2	103.5	100.5	3.4
Average		19.6	26.1	106.0	103.0	3.2
Verendrye 1	PS/86/20U21/453	18.7	23.3	110.8	109.2	1.6
Verendrye 2	"	19.0	25.4	107.7	106.2	1.6
Verendrye 3	"	17.9	23.3	109.5	107.2	1.5
Average		18.5	24.0	109.3	107.5	1.6
Virgin Creek 1	PS/86/20U17/374	20.4	25.8	105.7	104.2	1.4
Virgin Creek 2	"	20.6	26.2	104.5	103.4	1.1
Virgin Creek 3	"	23.3	25.5	101.4	99.4	1.9
Virgin Creek 4	"	21.9	27.0	103.3	100.9	2.3
Average		21.6	26.1	103.7	102.0	1.7
Mobridge 1	PS/86/20U13/295	20.1	24.5	109.1	106.8	2.2
Mobridge 2	"	17.5	24.1	109.5	106.5	2.8
Mobridge 3	"	17.5	23.6	109.0	104.6	4.4
Mobridge 4	PS/86/20U8/193	24.1	27.4	93.2	92.8	0.4
Mobridge 5	"	24.0	27.4	93.3	93.0	0.3
Average[a]		18.4	24.1	109.2	106.0	3.1
Elk Butte 1	PS/86/20U4/106	21.3	25.8	103.0	101.2	1.9
Elk Butte 2	"	17.7	25.5	107.3	104.8	2.3
Elk Butte 3	PS/87/19U7/172	21.8	26.0	102.7	100.1	2.6
Elk Butte 4	"	21.3	(b)	103.0	101.7	1.3
Average		20.5	25.8	104.0	102.0	2.0
Green River 1	GR/86/V34-0	0.56	0.58	133.1	133.1	0.0
Green River 2	"	0.60	0.63	139.5	139.5	0.0
Green River 3	"	0.59	0.60	139.9	139.9	0.0
Average		0.58	0.60	137.5	137.5	0.0
Rhinestreet 1	DR/86/160	1.20	1.60	165.5	164.4	0.7
Rhinestreet 2	"	1.50	2.00	168.1	167.3	0.2
Rhinestreet 3	"	1.20	1.70	169.3	168.8	0.4
Average		1.30	1.78	167.6	166.8	0.4

(a) Does not include Specimens 4 and 5 due to high organic content.
(b) Specimen damaged.

5.0 SUMMARY

The purpose of performing the tests discussed in this report is to increase the database for thermomechanical properties of different shale types. Testing of shale is a phase of an ongoing Repository Technology Program (RTP) of a much larger scope being conducted at Oak Ridge National Laboratory. The objective of the RTP is to assess tools and techniques that would be useful to evaluate a potential repository in a diversity of geologic and hydrologic settings. Shales constitute a large group of rock types being considered as a potential repository medium. Basic mechanical properties are needed for siting studies, design, and performance assessment. The diversity of rock types currently under consideration requires that different, fundamental properties of these rocks be evaluated and that the types of experiments conducted on each kind of rock will necessarily require different emphases.

The materials evaluated in this report represent several of the rock types that are conventionally classified and discussed in the literature as shales. This report is intended to be a data report which summarizes several properties of shales including mineralogy, strength, deformability, and durability. Each rock type has been examined by X-ray diffraction, principally to quantify the clay minerals and secondarily to provide a description of the composition of the entire rock. Clay minerals are particularly important because illitic shales are typically nonswelling and smectites are expandable. The Pierre Shale is a smectitic shale, while the Conasauga and Rhinestreet Shales contain mostly illitic clays. The Green River material contains only nominal amounts of clay, and, contrary to its misnomer, it cannot be classified as a shale.

Strength properties have been measured on these rock types and range from the weak Pierre Shale to the strong Rhinestreet Shale. The Pierre Shale averages 7.2 MPa and 0.5 MPa for unconfined compression and indirect tension, respectively. The unconfined compressive strength of Rhinestreet Shale averages 58.7 MPa, but the fissility prohibits testing by indirect tension or point load. The Green River material is much stronger in tension and compression at room temperature than any of the shales. A few unconfined compression tests at 150°C were conducted to assess the effects of elevated temperature. The Rhinestreet increased slightly in strength, and Green River dropped severely in strength owing to its kerogen content.

A relationship between mechanical results that may prove to be useful in future differentiation of rock types is the linearity between indirect tensile strength, point load index $I_s(50)$, and the unconfined compressive strength. These data are plotted in Figure 5-1 for three materials for which all three of these tests were run, including

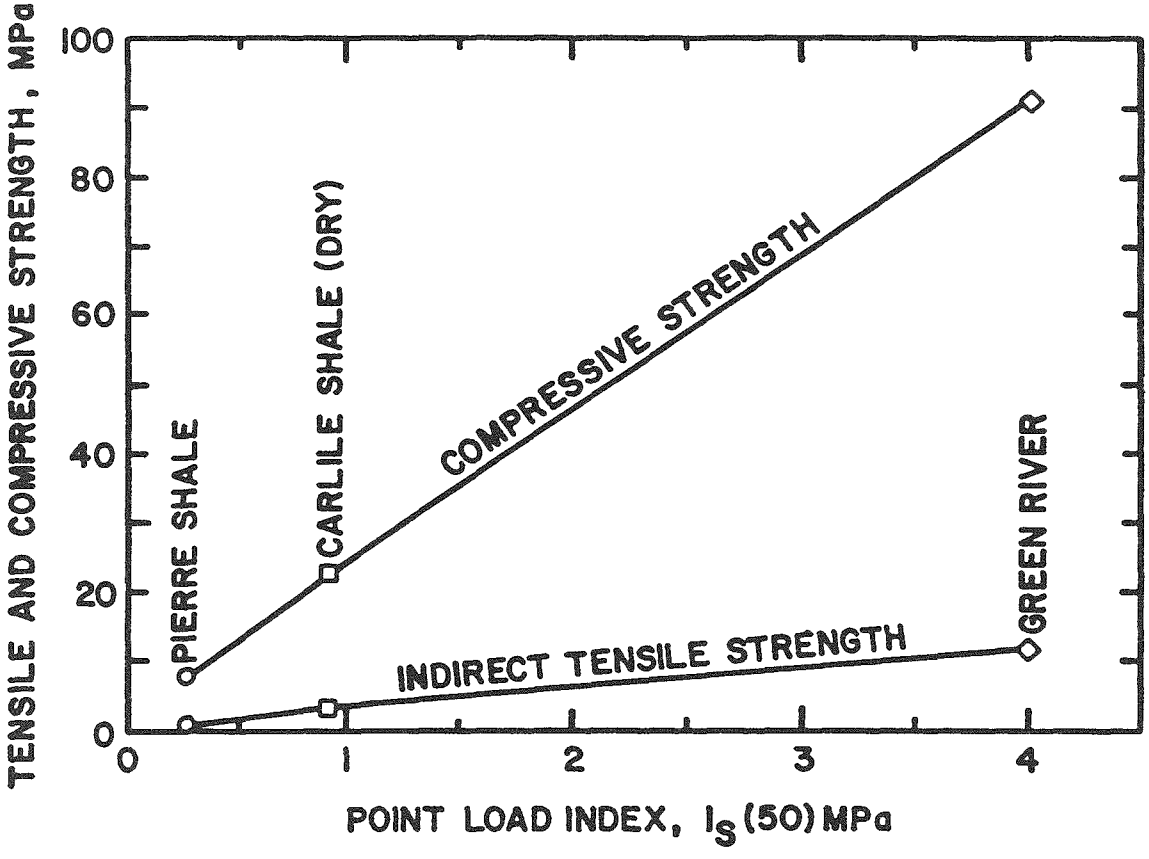

Figure 5-1. Point Load Index Plotted Against Tensile and Compressive Strength

Pierre Shale at natural moisture content, Carlile Shale in room-dry condition, and the Green River material. It appears that excellent estimates of other strength properties can be obtained if one (or two) of these tests is conducted. Because the shales are naturally very fissile, few competent specimens are usually available for testing. It may be important to be able to estimate strength properties by simple tests on small pieces of core.

The strength results are good indicators of index properties such as slake durability and swell. Neither Rhinestreet nor Green River was broken down after two cycles of slaking nor did these materials swell. The Pierre Shale is reduced to half its original weight after two cycles of slaking. The Pierre also swells and develops proportional swell pressures. The amount of swelling is correlated to the percentage of smectite.

The thermomechanical results summarized in this report demonstrate the feasibility of several test methods and potential application of certain index tests to differentiate between shale types even when a minimal amount of core is available.

6.0 REFERENCES

Abel, J. F., Jr., and D. W. Gentry, 1975. *Evaluation of Excavation Experience: Pierre Shale, ORNL/SUB-75/70347,* prepared for Office of Waste Isolation, Union Carbide Corporation, Nuclear Division, Oak Ridge, TN.

Blanton, T. L., S. A. Dischler, and N. C. Patti, 1981. *Mechanical Properties of Devonian Shales From the Appalachian Basin,* DOE/MC/08216-1332, prepared by Science Applications Inc., for United States Department of Energy, Morgantown Energy Technology Center, Morgantown, West Virginia.

Broch, E. and J. A. Franklin, 1972. "The Point-Load Strength Test," *International Journal of Rock Mechanics and Mining Sciences,* Vol. 9, pp. 669-697

Brown, E. T., 1981. *Rock Characterization Testing & Monitoring: ISRM Suggested Methods,* Pergamon Press, New York, NY.

Chong, K. P. and J. W. Smith, 1984. "Mechanical Characterization of Oil Shale," *Mechanics of Oil Shale,* K. P. Chong and J. W. Smith (eds), Elsevier Applied Science Publishers, New York, NY.

Chung, F. H., 1974a. "Quantitative Interpretation of X-Ray Diffraction Patterns of Mixtures. I: Matrix-Flushing Method for Quantitative Multi-Component Analysis," *Journal of Applied Crystallography,* Vol. 7, pp. 519-525.

Chung, F. H., 1974b. "Quantitative Interpretation of X-Ray Diffraction Patterns of Mixtures. II: Adiabatic Principle of X-Ray Diffraction Analysis of Mixtures," *Journal of Applied Crystallography,* Vol. 7, pp. 526-531.

Chung, F. H., 1975. "Quantitative Interpretation of X-Ray Diffraction Patterns of Mixtures. III: Simultaneous Determination of a Set of Reference Intensities," *Journal of Applied Crystallography,* Vol. 8, pp. 17-19.

Costin, L. S., 1980. "Material Properties of Oil Shale," SAND-81-1457, Sandia National Laboratories, Albuquerque, NM.

Croff, A. G., T. F. Lomenick, R. S. Lowrie, and S. H. Stow, 1987. *Evaluation of Five Sedimentary Rocks Other Than Salt for High-Level Waste Repository Siting Purposes,* ORNL-6241/V1,2,3, Oak Ridge National Laboratory, Oak Ridge, TN, June.

Davis, B. L., 1984. "Reference Intensity Quantitative Analysis Using Thin-Layer Aerosol Samples," *Advances in X-ray Analysis,* Vol. 27, Cohen, Russ, Leyden, Barrett, and Predecki (eds.), Plenum Publishing Corporation.

Davis, B. L., 1987. Senior Scientist, Institute of Atmospheric Sciences, South Dakota School of Mines and Technology, Rapid City, SD, Personal Communication to F. D. Hansen.

Davis, B. L. and M. J. Walawender, 1982. "Quantitative Mineralogical Analysis of Granitoid Rocks: A Comparison of X-Ray and Optical Techniques," *American Mineralogist,* Vol. 67, pp. 1135-1143.

DuBow, J., 1984. "Temperature Effects," *Mechanics of Oil Shale,* K. P. Chong and J. W. Smith (eds.), Elsevier Applied Science Publishers, New York, pp. 523-578.

Franklin, J. A. and R. Chandra, 1972. "The Slake Durability Test," *International Journal of Rock Mechanics and Mining Sciences,* Vol. 9, pp. 325-341.

Gamble, J. C., 1971. *Durability-Plasticity Classification of Shales and Other Argillaceous Rocks,* Ph.D. Thesis, University of Illinois, Urbana/Champaign, IL.

ISRM, 1985. "Suggested Method for Determining Point Load Strength," *International Journal of Rock Mechanics and Mining Science and Geomechanical Abstracts,* Vol. 22, No. 2, pp. 51-60.

Lambe, T. W., 1951. *Soil Testing for Engineers,* John Wiley and Sons, Inc., New York, NY.

Mutter, F. H., 1984. *RE/SPEC Inc. Quality Assurance Manual,* prepared by RE/SPEC Inc., Rapid City, SD, RSI-0272, for Office of Nuclear Waste Isolation, Battelle Memorial Institute, Columbus, OH, October.

Petry, T. M. and J. C. Armstrong, 1980. "Relationships and Variations of Properties of Clay," *Proceedings of the Fourth International Conference on Expansive Soils,* Denver, Colorado, Vol. 1, pp. 172-189, June.

Pettijohn, F. J., 1975. *Sedimentary Rocks,* Harper and Row, Publishers, New York, NY.

Schultz, L. G., 1978. *Mixed-Layer Clay in the Pierre Shale and Equivalent Rocks, Northern Great Plains Region,* Geological Survey Professional Paper 1064-A, United States Government Printing Office, Washington, DC.

APPENDIX A

UNCONFINED COMPRESSION TESTS ON SHALES: STRESS-STRAIN CURVES AT ROOM TEMPERATURE

APPENDIX A
LIST OF FIGURES

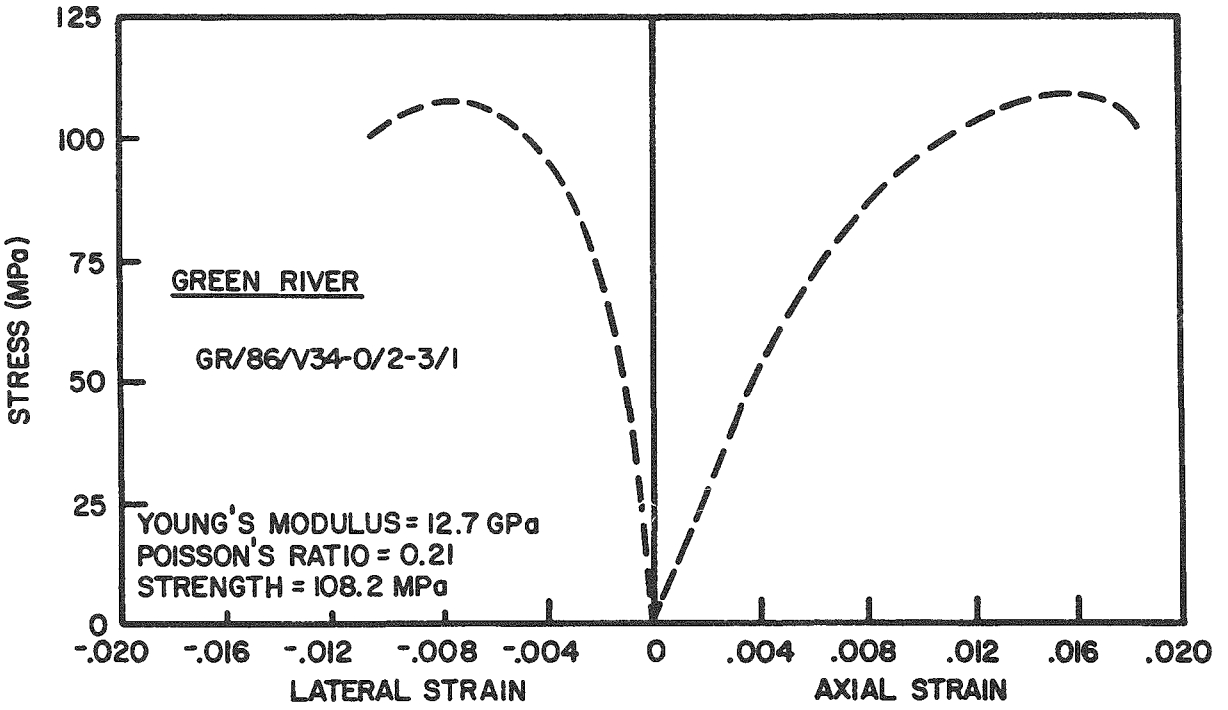

Figure A-1. Stress-Strain Curves for Room Temperature: Unconfined Compression Tests on Green River Specimen GR/86/V34-0/2-3/1

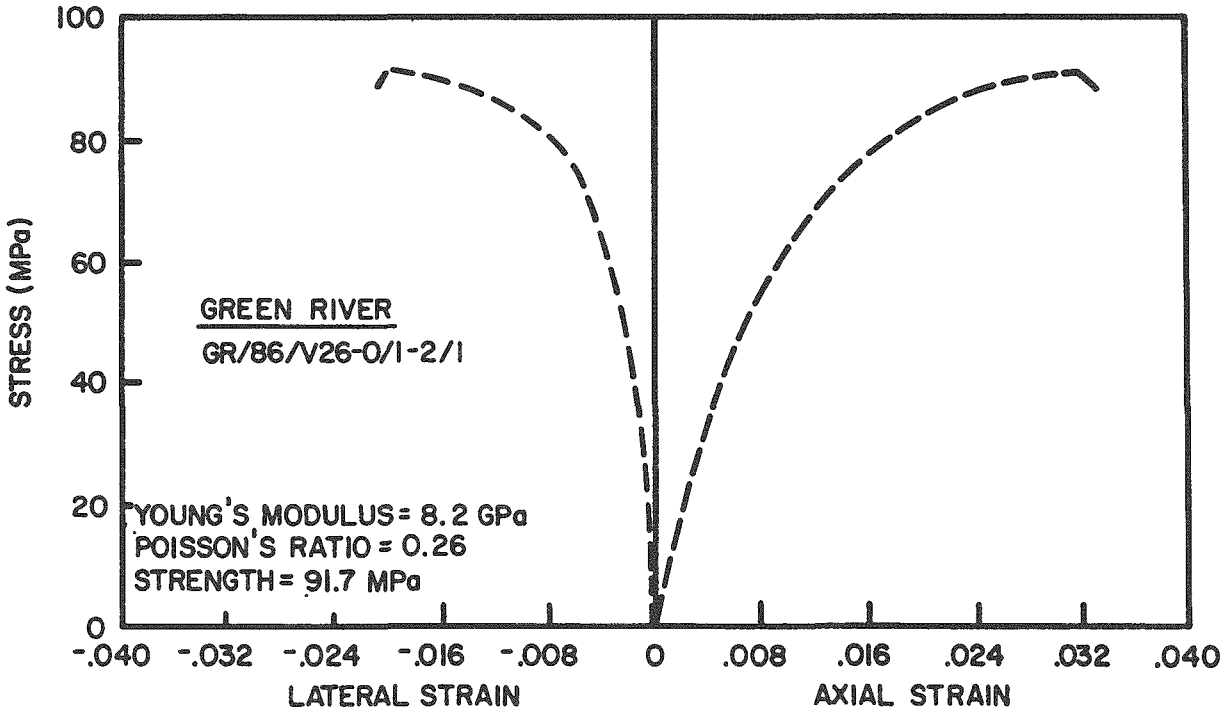

Figure A-2. Stress-Strain Curves for Room Temperature: Unconfined Compression Tests on Green River Specimen GR/86/V26-0/1-2/1

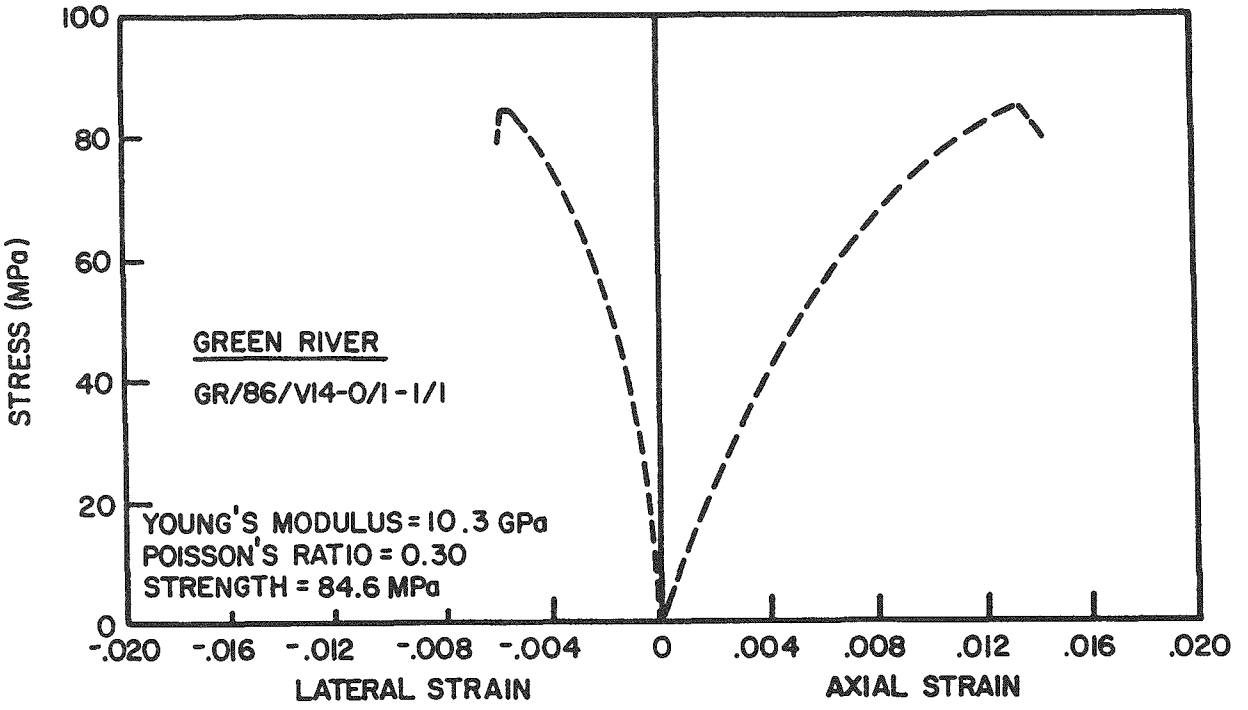

Figure A-3. Stress-Strain Curves for Room Temperature: Unconfined Compression Tests on Green River Specimen GR/86/V14-0/1-1/1

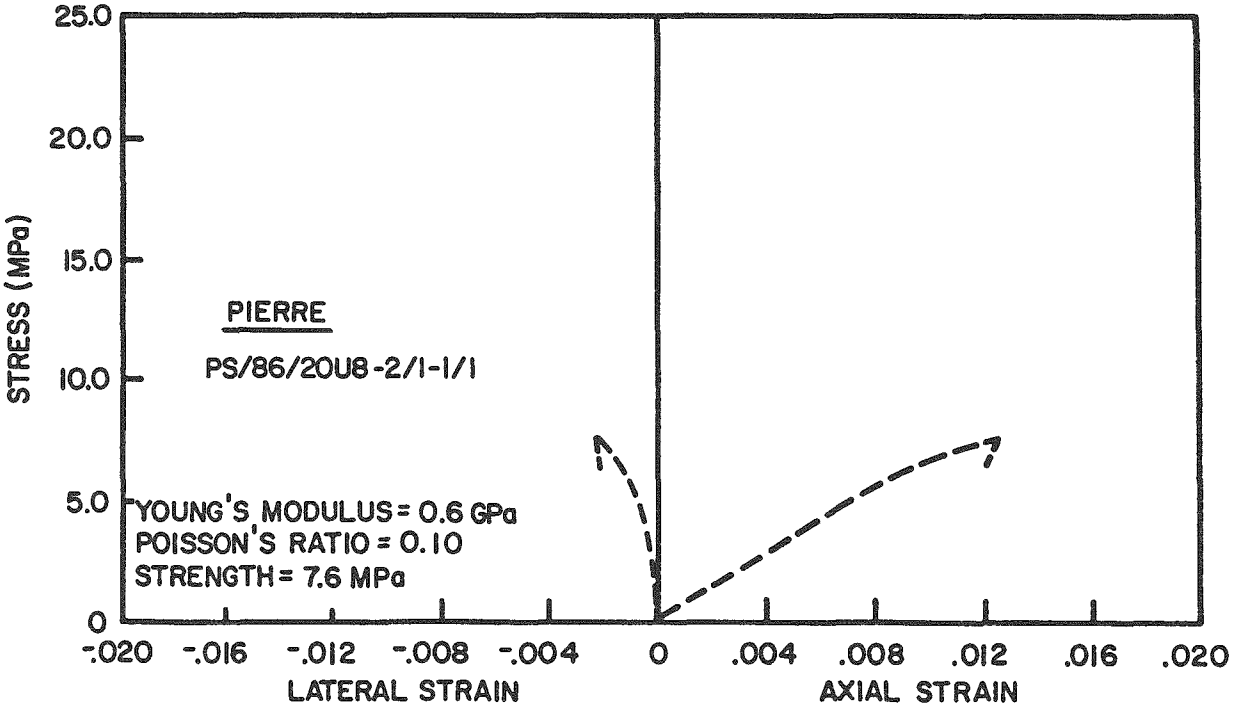

Figure A-4. Stress-Strain Curves for Room Temperature: Unconfined Compression Tests on Pierre Specimen PS/86/20U8-2/1-1/1

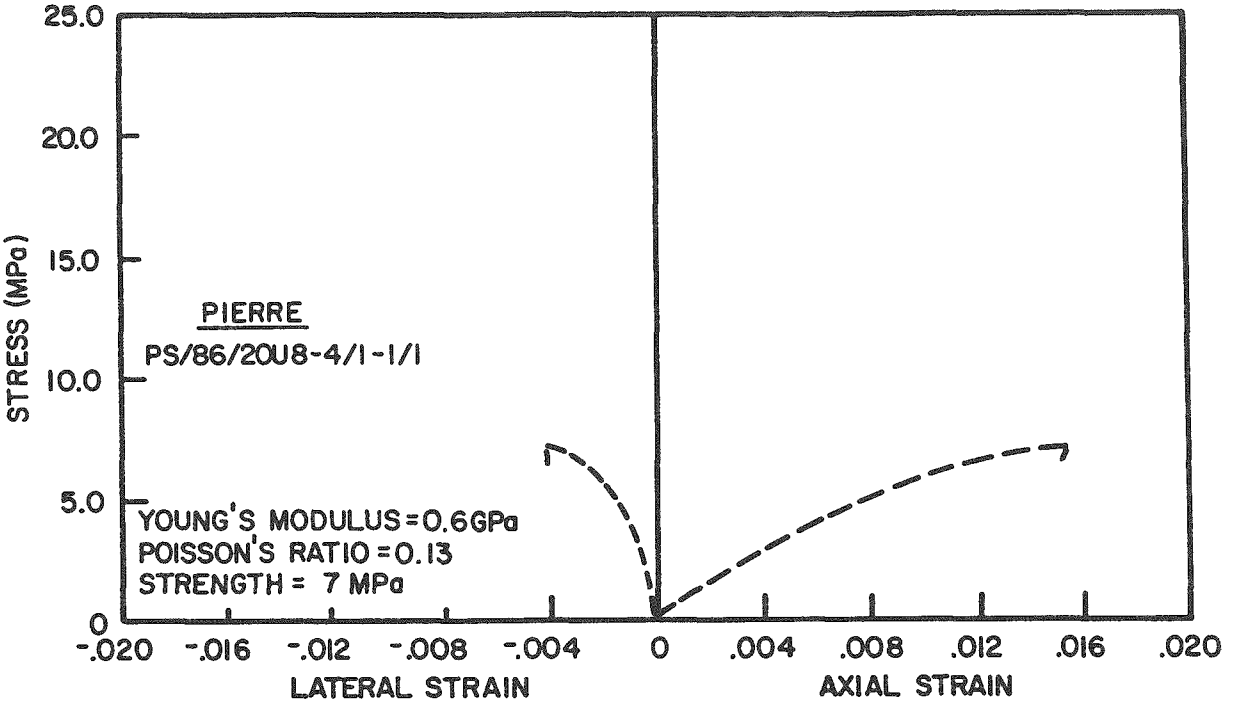

Figure A-5. Stress-Strain Curves for Room Temperature: Unconfined Compression Tests on Pierre Specimen PS/86/20U8-4/1-1/1

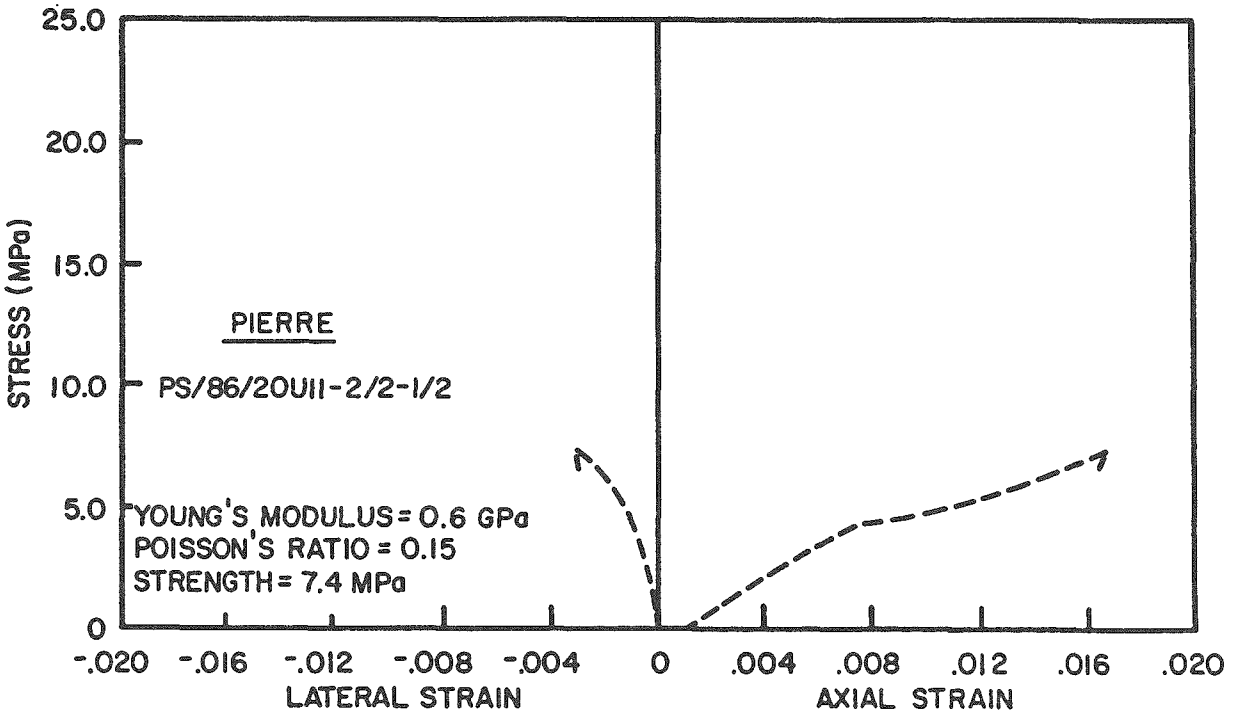

Figure A-6. Stress-Strain Curves for Room Temperature: Unconfined Compression Tests on Pierre Specimen PS/86/20U11-2/2-1/2

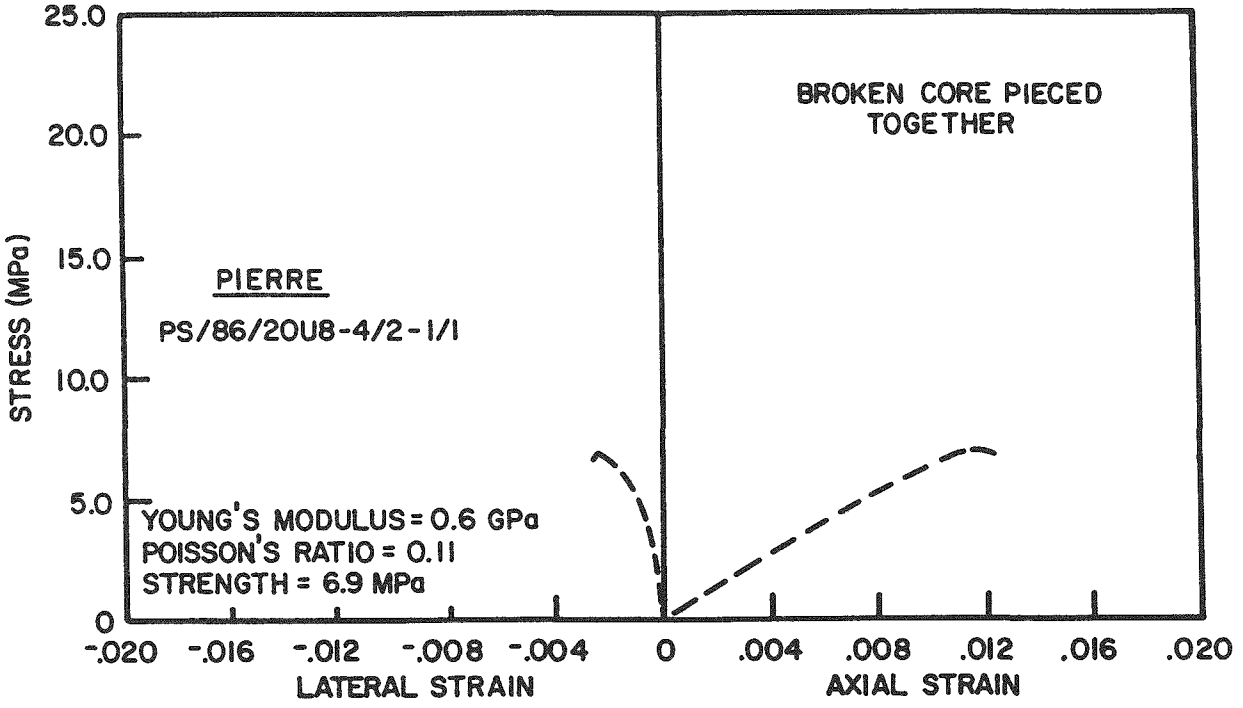

Figure A-7. Stress-Strain Curves for Room Temperature: Unconfined Compression Tests on Pierre Specimen PS/86/20U8-4/2-1/1

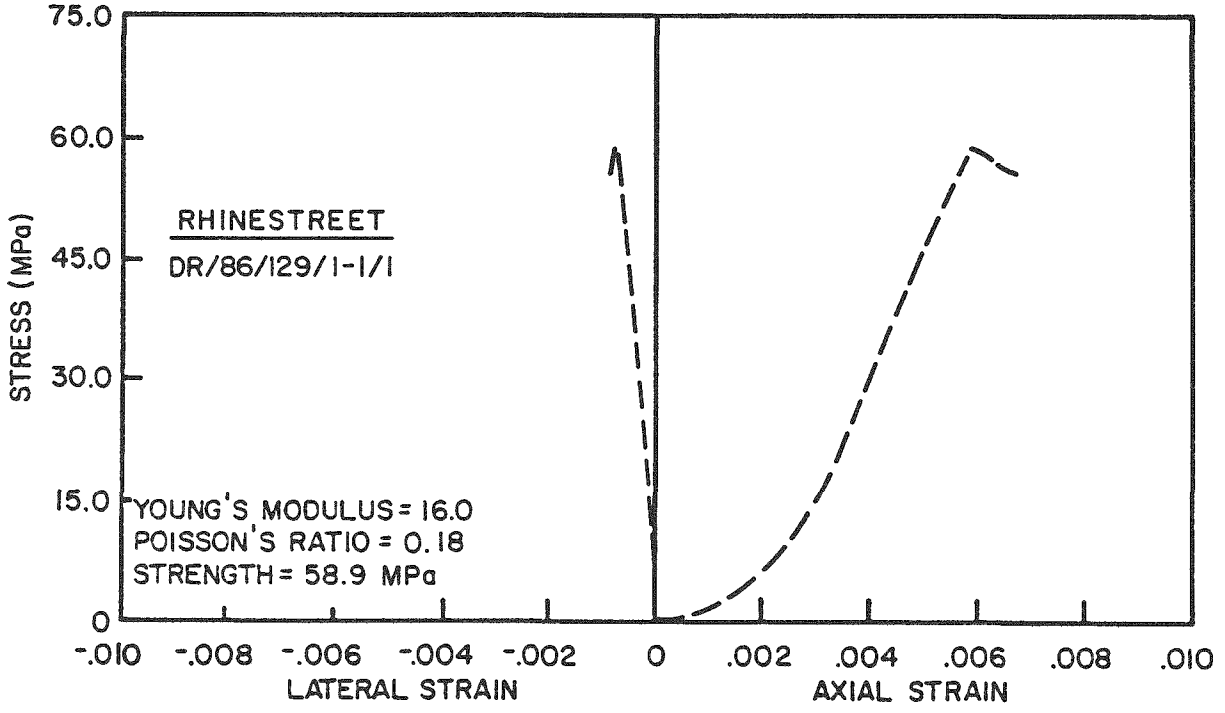

Figure A-8. Stress-Strain Curves for Room Temperature: Unconfined Compression Tests on Rhinestreet Specimen DR/86/129/1-1/1

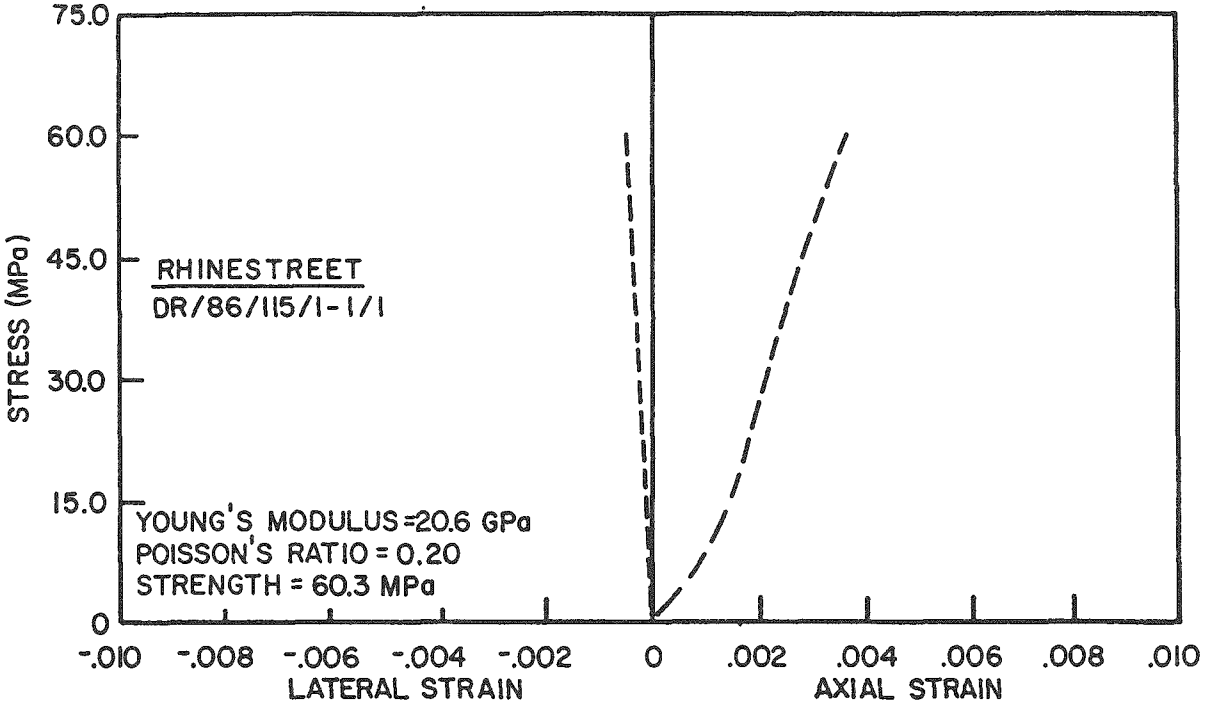

Figure A-9. Stress-Strain Curves for Room Temperature: Unconfined Compression Tests on Rhinestreet Specimen DR/86/115/1-1/1

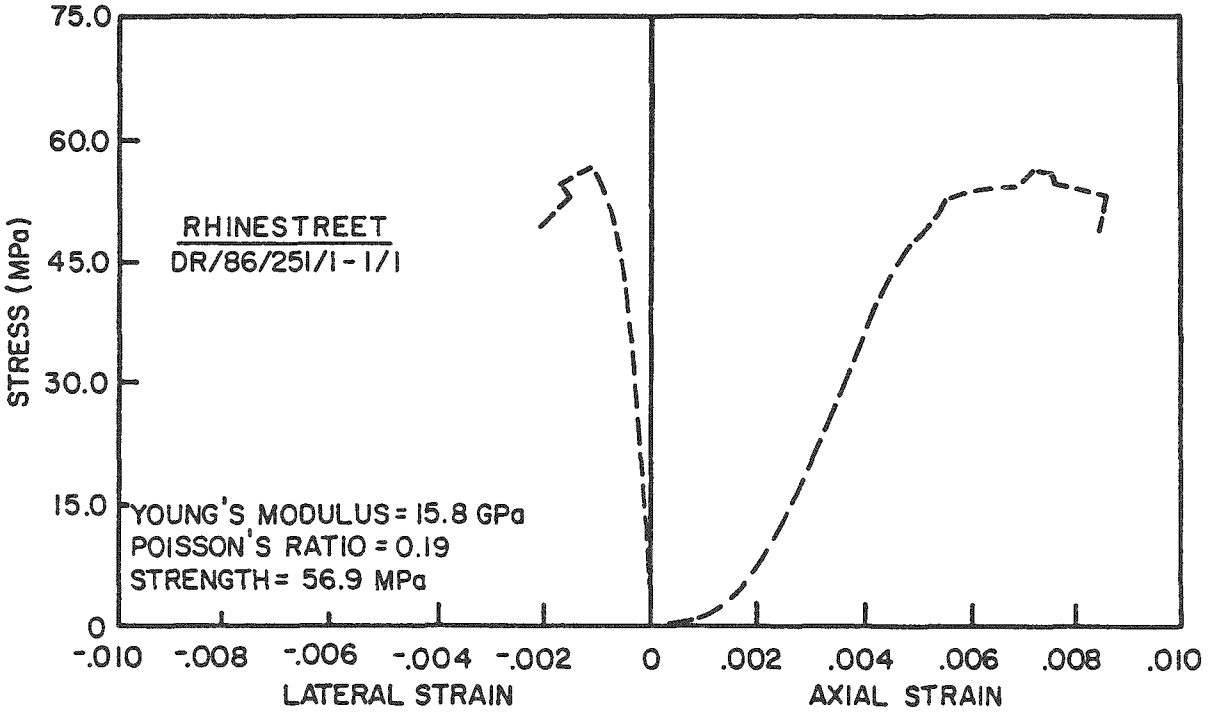

Figure A-10. Stress-Strain Curves for Room Temperature: Unconfined Compression Tests on Rhinestreet Specimen DR/86/251/1-1/1

RSI-087-86-15

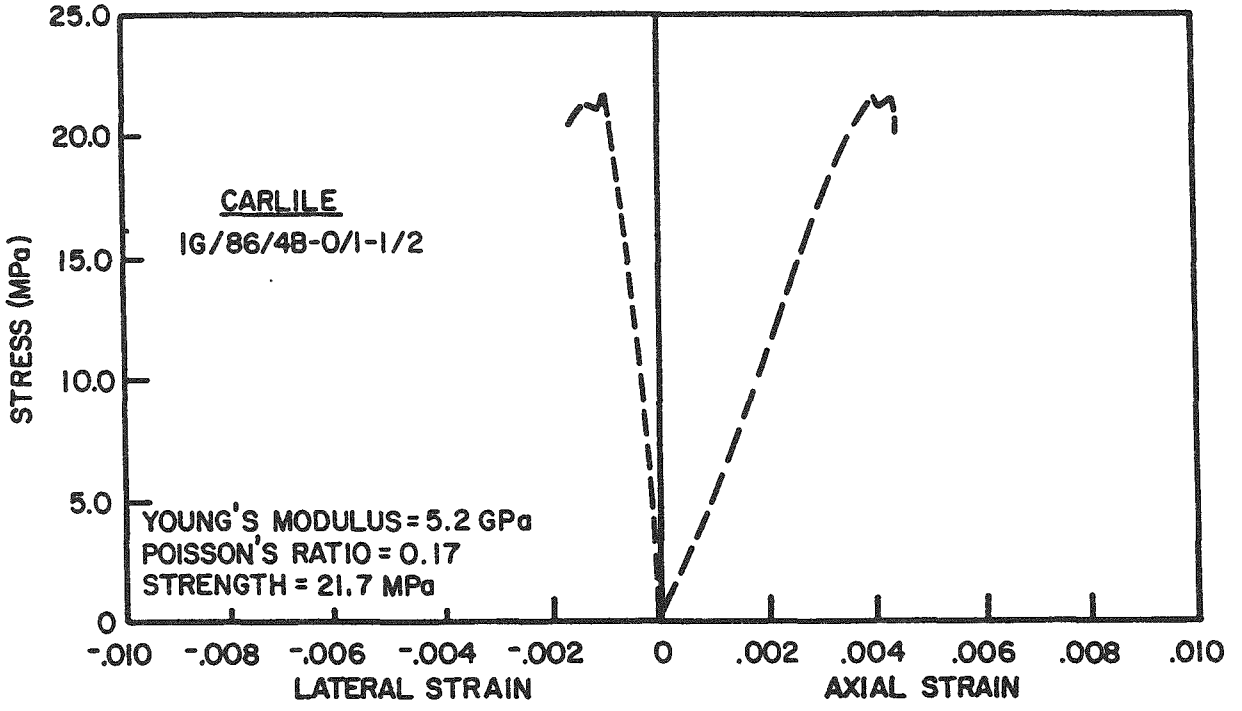

Figure A-11. Stress-Strain Curves for Room Temperature: Unconfined Compression Tests on Carlile Specimen IG/86/4B-0/1-1/2

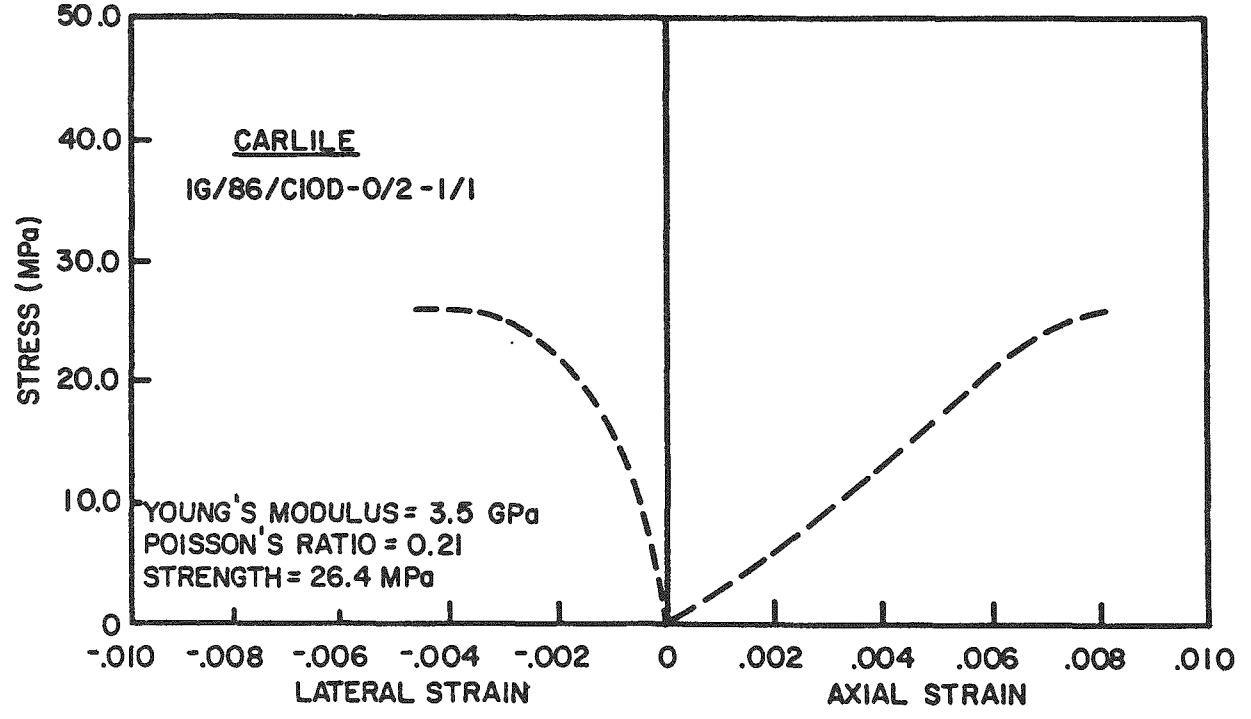

Figure A-12. Stress-Strain Curves for Room Temperature: Unconfined Compression Tests on Carlile Specimen IG/86/C10D-0/2-1/1

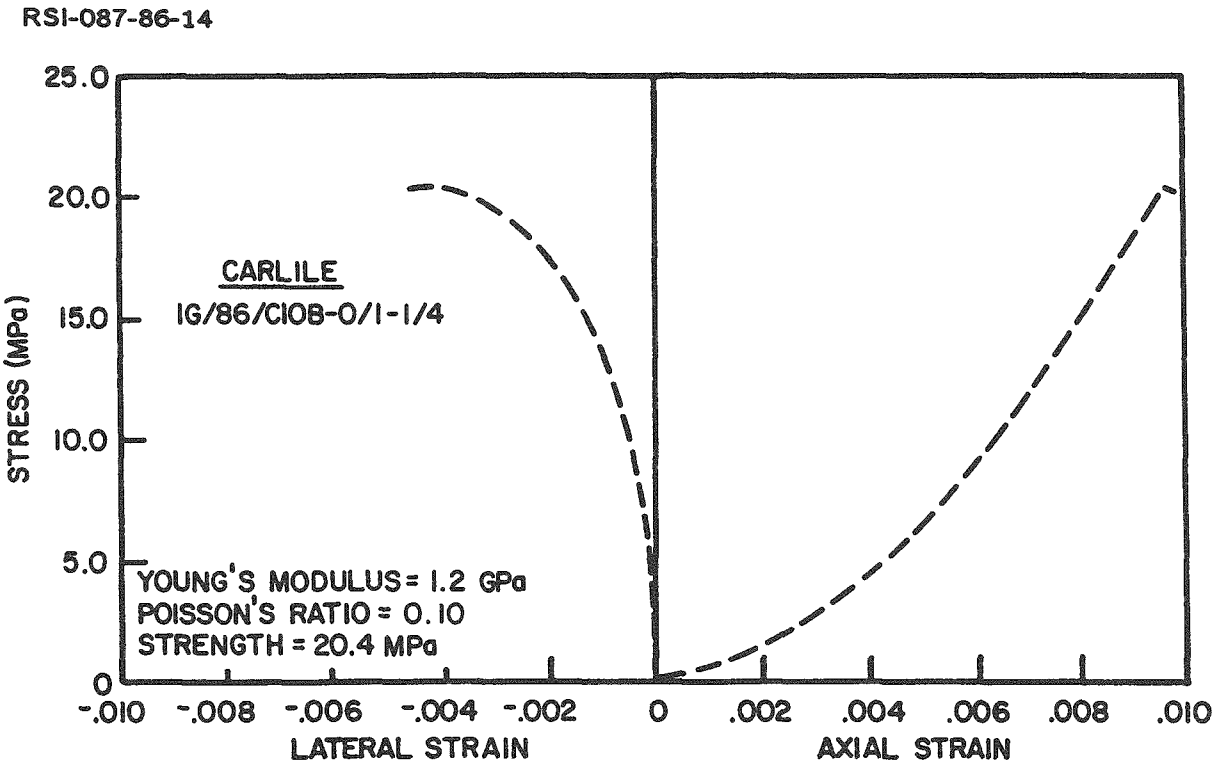

Figure A-13. Stress-Strain Curves for Room Temperature: Unconfined Compression Tests on Carlile Specimen IG/86/C10B-0/1-1/4

APPENDIX B

UNCONFINED COMPRESSION TESTS ON SHALES: STRESS-STRAIN CURVES AT 150°C

APPENDIX B
LIST OF FIGURES

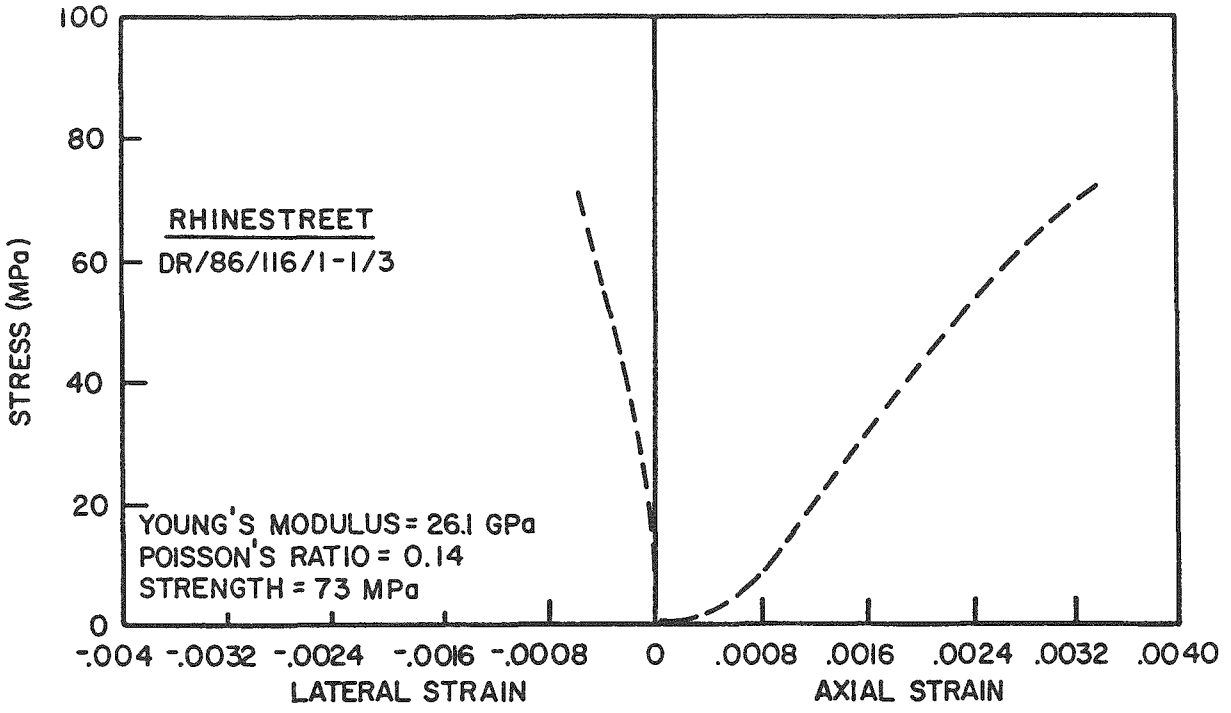

Figure B-1. Stress-Strain Curves for Unconfined Compression Tests on Rhinestreet Specimen DR/86/116/1-1/3 at 150°C

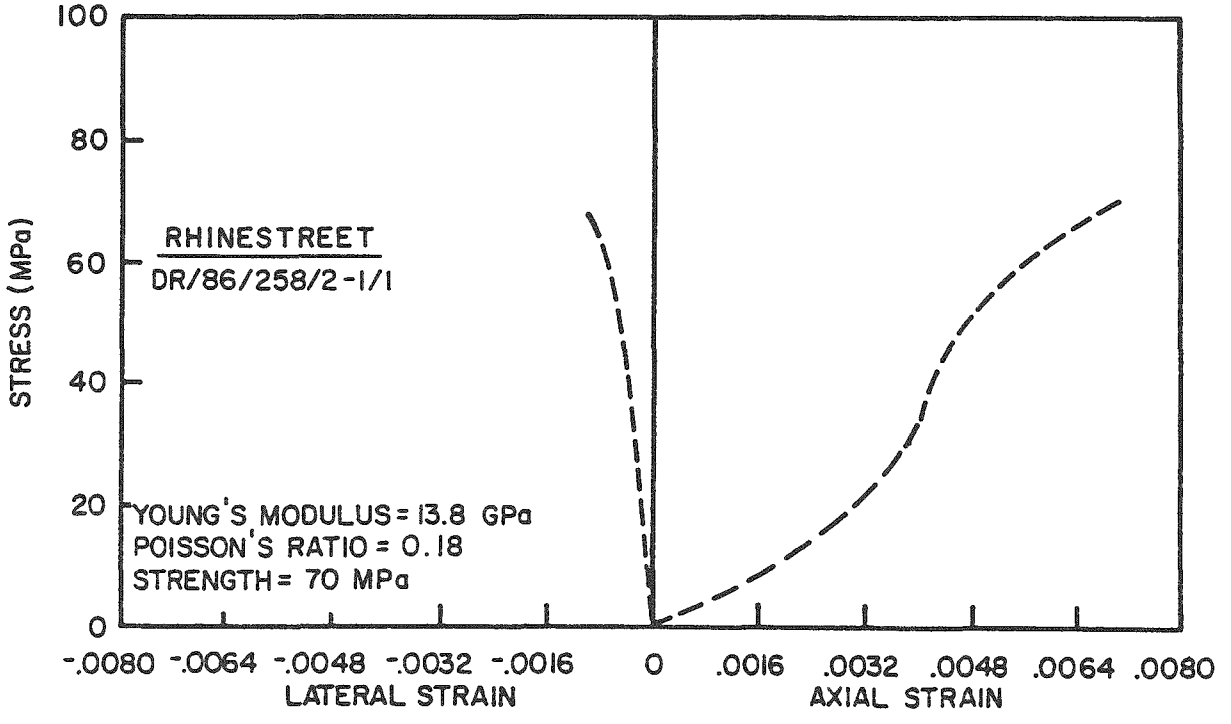

Figure B-2. Stress-Strain Curves for Unconfined Compression Tests on Rhinestreet Specimen DR/86/258/2-1/1 at 150°C

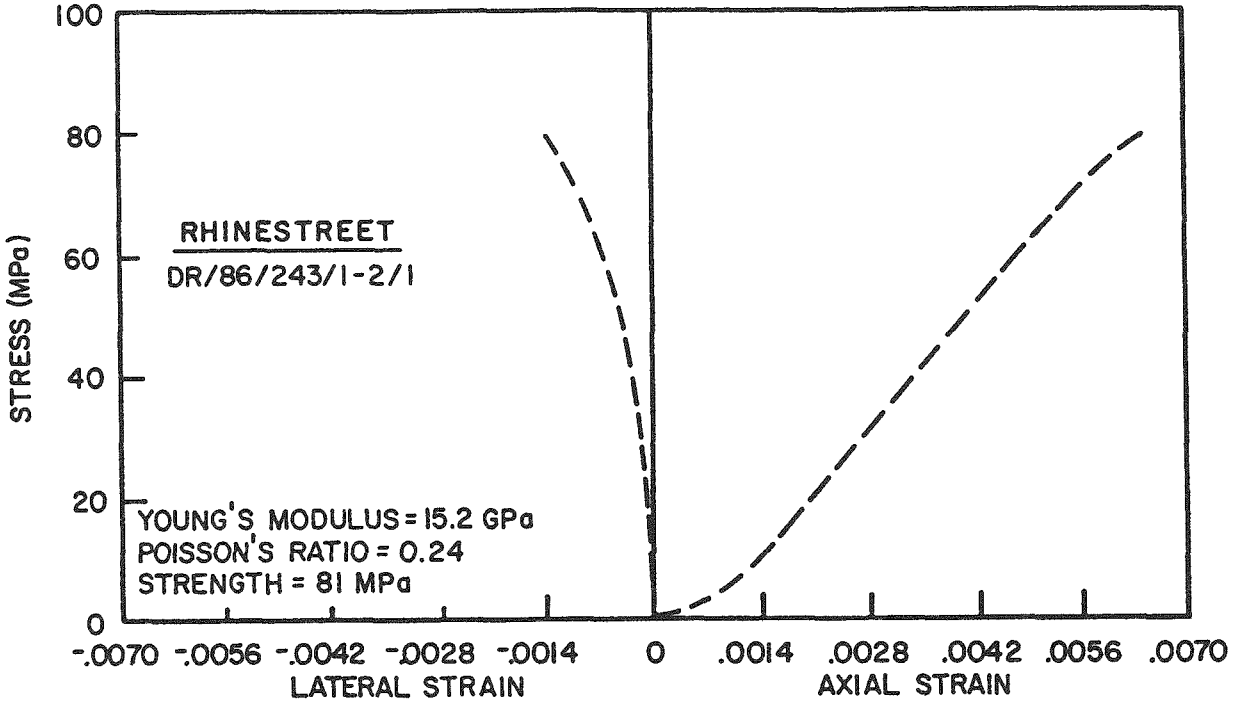

Figure B-3. Stress-Strain Curves for Unconfined Compression Tests on Rhinestreet Specimen DR/86/243/1-2/1 at 150°C

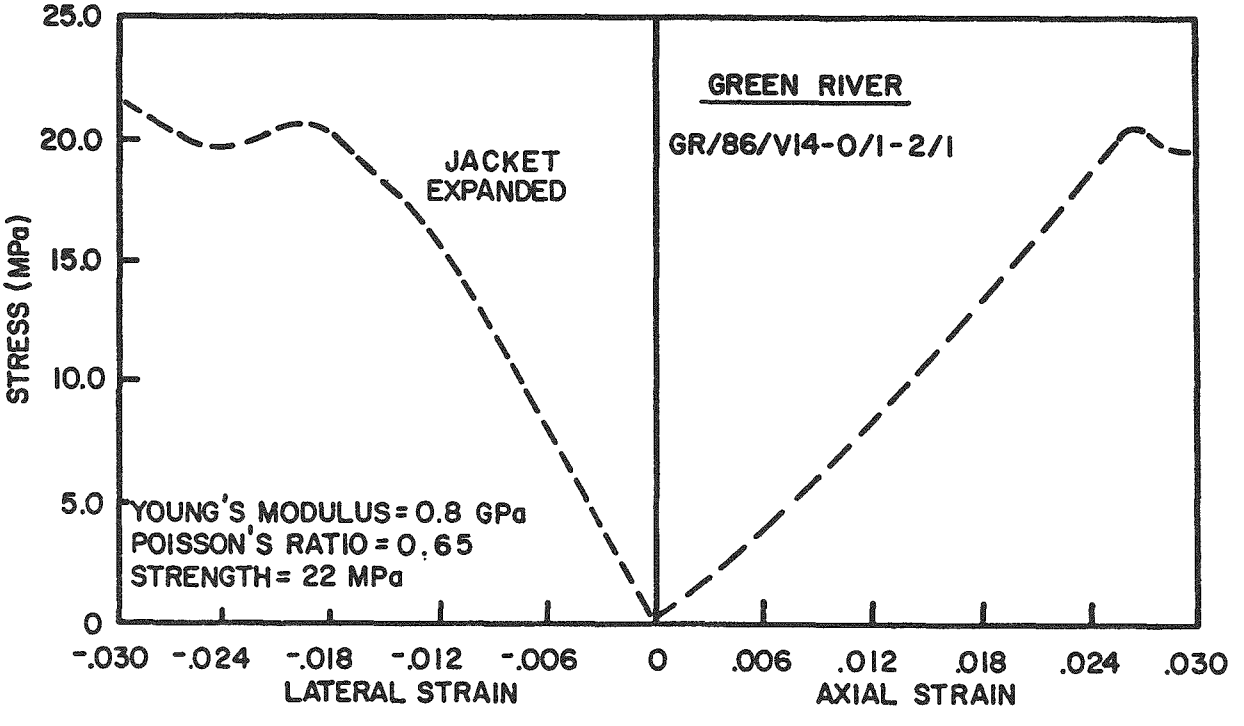

Figure B-4. Stress-Strain Curves for Unconfined Compression Tests on Green River Specimen GR/86/V14-0/1-2/1 at 150°C

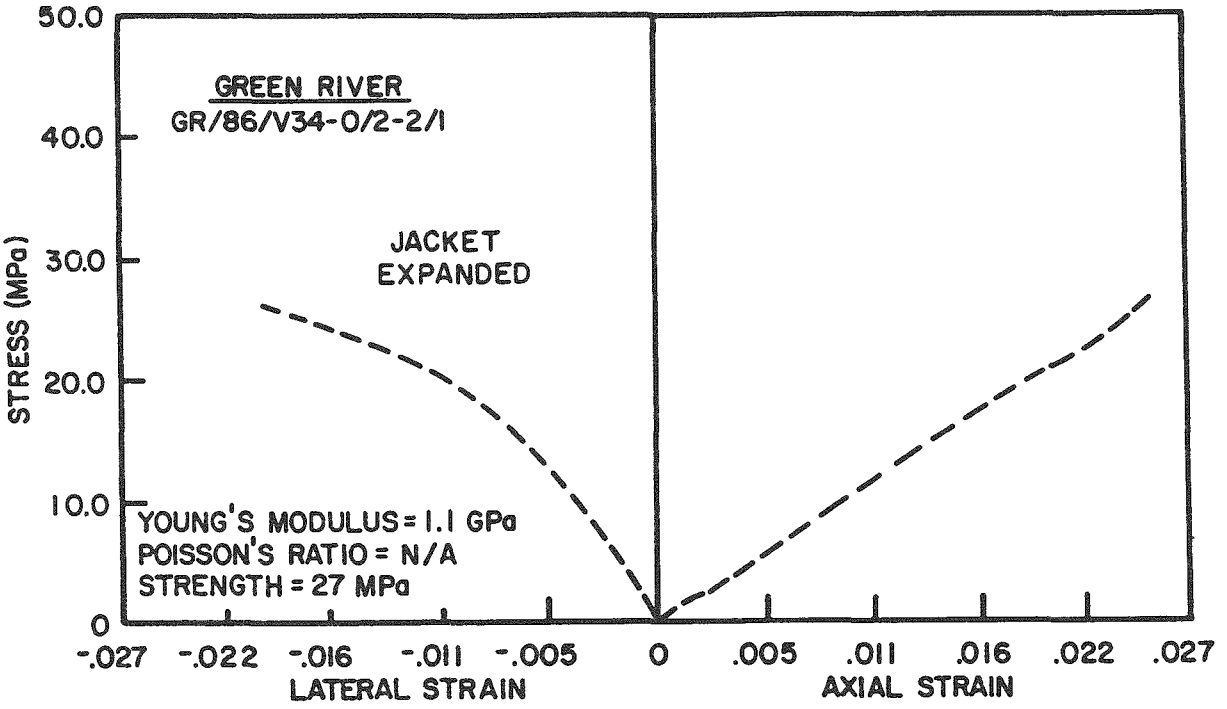

Figure B-5. Stress-Strain Curves for Unconfined Compression Tests on Green River Specimen GR/86/V34-0/2-2/1 at 150°C

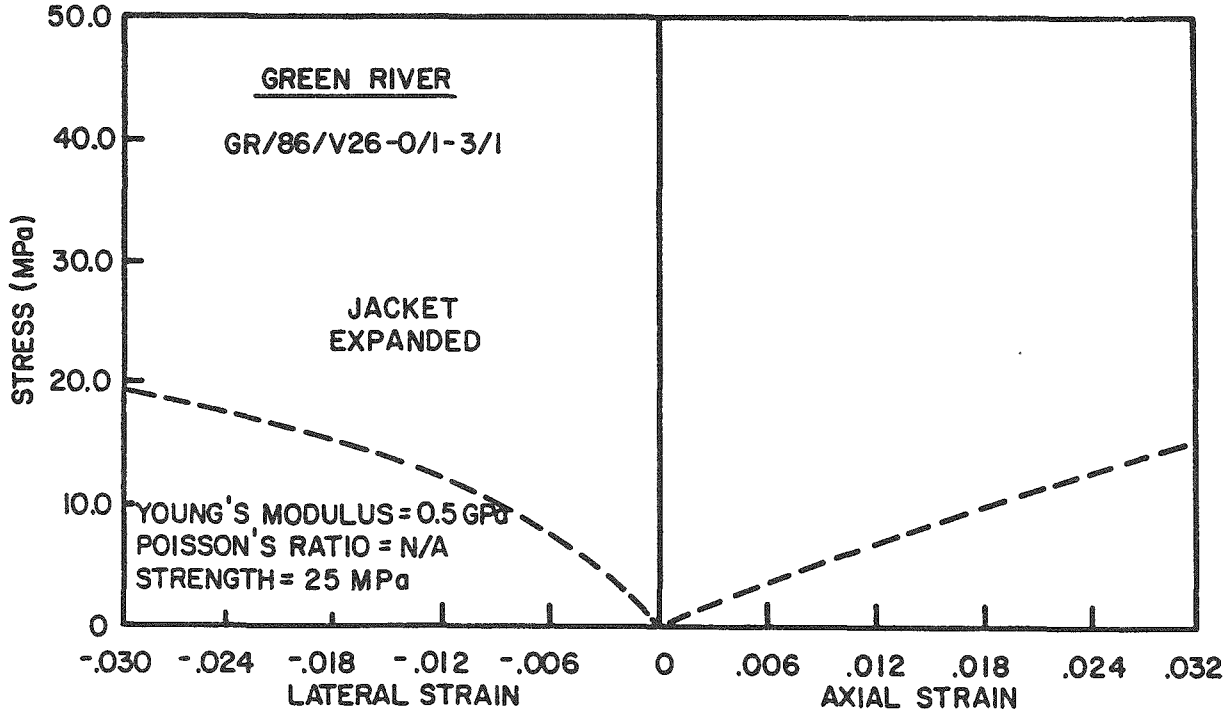

Figure B-6. Stress-Strain Curves for Unconfined Compression Tests on Green River Specimen GR/86/V26-0/1-3/1 at 150°C

APPENDIX C

INDIRECT TENSILE STRENGTH OF SHALES

APPENDIX C
LIST OF TABLES

Table C-1. Indirect Tensile Strength of Carlile Shale

Shale Type	Specimen Identification	Length (inches)	Diameter (inches)	Load (kN)	Tensile Strength (MPa)
Carlile	IG/86/4B-0/1-1/1[a]	1.052	2.004	4.55	2.13
	IG/86/C8B-1/1-1/1/2-1[a,b]	1.069	2.001	5.69	2.63
	IG/86/C10B-0/1-1/2[a]	1.065	1.984	7.47	3.49
	IG/86/C8B-1/1-1/1/3-1[a,b]	1.038	2.000	4.67	2.22
	IG/86/C8B-1/1-1/1/1-1[a,b]	1.057	2.000	7.64	3.57
	IG/86/C10D-0/2-1/2[a]	0.998	1.998	6.74	3.34
	IG/86/C8B-1/2-1/2[a]	1.026	1.991	6.73	3.25
	IG/86/C10C-0/2-1/2[a]	1.051	2.005	5.57	2.61
	IG/86/4D-0/1-1/2[a]	1.085	2.000	19.41	8.83
	IG/86/1B-0/1-1/1	1.060	1.975	6.44	3.03
	IG/86/1B-0/1-2/1	1.072	1.975	5.97	2.78
	IG/86/C10D-0/2-1/3	1.020	1.980	6.54	3.19
	IG/86/1A-0/1-1/3	1.055	1.988	10.34	4.86
	IG/86/C8B-1/2-1/1	1.042	1.988	7.34	3.50
	IG/86/1A-0/1-1/1	1.047	1.970	8.78	4.20
	IG/86/1A-0/1-1/4	1.014	1.989	7.06	3.49
	IG/86/C8B-0/1-3/1	1.074	1.988	5.54	2.56
	IG/86/C8B-0/1-2/1	1.049	1.992	5.89	2.78

(*a*) Curved platens—all others straight platens.
(*b*) Broken but usable.

Table C-2. Indirect Tensile Strength of Green River Formation

Shale Type	Specimen Identification	Length (inches)	Diameter (inches)	Load (kN)	Tensile Strength (MPa)
Green River	GR/86/V43-0/1-2/2[a]	1.057	1.999	23.05	10.77
	GR/86/V43-0/1-2/3[a]	1.052	1.999	31.32	14.70
	GR/86/V43-0/1-2/4[a]	1.050	1.999	26.62	12.52
	GR/86/V43-0/1-3/2T[a]	1.043	1.998	24.23	11.47
	GR/86/V43-0/1-3/2B[a]	0.943	1.999	26.03	13.67
	GR/86/V43-0/1-4/2[a]	1.043	1.998	25.51	12.07
	GR/86/V43-0/1-4/3[a]	1.058	1.999	30.98	14.45
	GR/86/V43-0/1-4/4[a]	1.056	1.998	34.89	16.31
	GR/86/V34-0/1-1/2[a]	1.064	1.999	27.96	12.93
	GR/86/V34-0/1-2/2[a]	1.053	1.999	26.89	12.61
	GR/86/V34-0/1-3/2[a]	1.042	2.000	28.67	13.58
	GR/86/V34-0/1-4/2	1.059	2.000	16.17	7.59
	GR/86/V34-0/2-1/2	1.045	2.000	18.87	8.91
	GR/86/V34-0/2-2/2	1.056	2.000	27.76	12.97
	GR/86/V34-0/2-3/2	1.055	1.999	24.43	11.43
	GR/86/V34-0/2-4/2	1.056	2.000	18.97	8.87
	GR/86/V26-0/1-2/2	1.034	1.999	31.80	15.18
	GR/86/V26-0/1-3/2	1.054	1.999	24.69	11.61
	GR/86/V26-0/1-4/2	1.057	1.999	23.05	10.76
	GR/86/V33-0/2-3/2	1.072	1.999	25.98	11.97
	GR/86/V53-0/1-3/1	1.069	2.000	23.35	10.78
	GR/86/V53-0/1-3/2	1.049	2.000	14.42	6.75

(*a*) Curved platens—all others straight platens.

Table C-3. Indirect Tensile Strength of Rhinestreet Shale

Shale Type	Specimen Identification	Length (inches)	Diameter (inches)	Load (kN)	Tensile Strength (MPa)
Rhinestreet	DR/86/259/1-1/2[a]	1.016	1.977	16.50	8.11
	DR/86/259/1-1/1[a]	1.025	1.974	10.47	5.10
	DR/86/144/1-1/3[a]	1.039	1.980	12.41	5.96
	DR/86/144/1-1/2[a]	1.055	1.980	18.35	8.67
	DR/86/256/1-1/2[a]	1.132	1.980	15.46	6.81
	DR/86/198/1-1/3[a]	1.043	1.997	19.28	9.13
	DR/86/260/1-1/3[a]	1.036	1.979	11.95	5.75
	DR/86/260/1-1/2[a]	1.101	1.984	20.99	9.48
	DR/86/160/1-1/1[a]	1.030	1.996	17.40	8.35
	DR/86/160/1-1/2	1.038	1.997	16.14	7.68
	DR/86/160/1-1/3	1.043	1.997	16.25	7.70
	DR/86/174/2-1/2	1.069	1.975	16.40	7.66
	DR/86/202/1-1/2	1.053	1.997	19.31	9.06
	DR/86/202/1-1/3	1.025	1.997	15.67	7.56
	DR/86/132/1-1/2	1.069	1.997	13.03	6.02
	DR/86/120/1-1/1	1.015	1.998	25.16	12.24
	DR/86/267/1-1/3	1.041	1.985	19.41	9.27
	DR/86/267/1-1/1[b]	1.062	1.982	—	—

(*a*) Curved platens—all others straight platens.
(*b*) Ran out of stroke.

Table C-4. Indirect Tensile Strength of Pierre Shale

Shale Type	Specimen Identification	Length (inches)	Diameter (inches)	Load (kN)	Tensile Strength (MPa)
Pierre	PS/86/20U7-0/2-1/1[c]	1.564	2.999	—	—
	PS/86/20U7-0/2-1/2	1.593	2.999	1.98	0.61
	PS/86/20U7-0/2-1/3	1.568	2.999	1.46	0.31
	PS/86/20U13-3B/1T-1/1	1.502	3.007	2.27	0.50
	PS/86/20U13-1T/1-1/1	1.503	3.002	2.23	0.49
	PS/86/20U13-1T/2-1/1	1.495	3.005	2.54	0.56
	PS/86/20U13-3T/2-1/1	1.501	3.004	2.32	0.51
	PS/86/20U13-3T/1-1/1	1.502	3.007	2.78	0.61
	PS/86/20U7-0/4-1/1	1.544	3.001	2.56	0.55
	PS/86/20U7-0/4-1/2	1.538	3.001	2.75	0.59
	PS/86/20U7-0/4-1/3	1.564	3.001	1.50	0.31
	PS/86/20U7-0/4-1/4	1.618	3.001	2.52	0.51
	PS/86/20U7-0/5-1/1	1.587	2.999	2.41	0.50
	PS/86/20U7-0/5-1/2	1.542	2.999	2.02	0.43
	PS/86/20U7-0/5-1/3	1.545	2.999	2.00	0.43
	PS/86/20U7-0/5-1/4	1.525	2.999	2.52	0.54
	PS/86/20U10-0/2-1/1	1.563	2.951	3.55	0.76
	PS/86/20U10-0/2-1/2	1.580	2.951	3.90	0.83

(c) Ran out of stroke.

APPENDIX D

POINT LOAD INDEXES OF SHALES

APPENDIX D
LIST OF TABLES

Table D-1. Point Load Index: Pierre Shale

Test	Platen Distance (inches)	Diameter of Core (inches)	1/2 Length of Core	Point Load Index $I_s(50)$	
				(psi)	(MPa)
AXIAL					
PS/86/19U7-3A	1.627	2.427	NA	30.99	0.214
PS/86/19U7-3B	1.966	2.427	NA	21.30	0.147
PS/86/20U10-0/2-1-3A	1.025	2.968	NA	60.77	0.419
PS/86/20U10-0/2-1-3B	1.666	2.968	NA	49.68	0.343
PS/86/20U10-0/3-1/B	1.566	2.920	NA	24.84	0.171
PS/86/20U10-0/4-1A	1.464	3.028	NA	25.15	0.173
PS/86/20U10-0/4-1C	2.162	2.911	NA	19.83	0.137
PS/86/20U10-0/4-1D	1.872	2.911	NA	17.25	0.119
PS/86/1A[(a)]	0.930	1.919	NA	64.37	0.444
PS/86/1B[(a)]	1.149	1.999	NA	31.76	0.219
PS/86/20U11-2/3-1A	0.740	2.025	NA	26.80	0.185
PS/86/20U11-2/3-1F	1.000	2.025	NA	47.76	0.329
PS/86/20U15-4A	1.360	3.035	NA	18.95	0.131
PS/86/20U15-3C	1.484	2.936	NA	61.83	0.426
PS/86/20U15-3D	1.841	2.945	NA	62.83	0.433
PS/86/20U15-2C	2.089	2.963	NA	44.20	0.305
PS/86/20U15-2E	1.251	2.927	NA	49.96	0.345
Average				38.72	0.267
DIAMETRAL					
PS/86/19U7-3	2.427	NA	3.5	25.45	0.176
PS/86/20U15-3A	2.975	NA	4.2	30.40	0.210
PS/86/20U15-1A	2.918	NA	3.2	14.72	0.101
PS/86/20U15-1C	3.010	NA	2.8	21.44	0.148
PS/86/20U5-6	2.888	NA	3.2	4.49	0.031
Average				19.30	0.133

(*a*) Original identification numbers were obscured.

Table D-2. Point Load Index: Green River Formation

Test	Platen Distance (inches)	Diameter of Core (inches)	1/2 Length of Core	Point Load Index $I_s(50)$	
				(psi)	(MPa)
AXIAL					
GR/86/4	1.353	1.999	NA	623.32	4.299
GR/86/6	1.365	1.999	NA	610.64	4.211
GR/86/7	0.928	1.999	NA	528.18	3.643
GR/86/11	1.328	1.999	NA	602.28	4.154
GR/86/12	1.065	1.999	NA	622.74	4.295
GR/86/13	1.566	1.999	NA	620.91	4.282
GR/86/18	1.441	1.999	NA	557.26	3.843
GR/86/19	1.272	1.999	NA	524.87	3.620
GR/86/20	1.324	1.999	NA	461.39	3.182
GR/86/21	1.060	1.999	NA	666.01	4.593
GR/86/25	1.160	1.999	NA	625.84	4.316
GR/86/26	1.248	1.999	NA	573.30	3.954
GR/86/27	1.526	1.999	NA	529.19	3.650
GR/86/28	1.107	1.999	NA	604.35	4.168
Average				582.20	4.015
DIAMETRAL					
GR/86/1	1.999	NA	2.50	351.40	2.423
GR/86/2	1.999	NA	1.25	415.64	2.866
GR/86/3	1.999	NA	1.25	290.95	2.007
GR/86/8	1.999	NA	2.50	226.71	1.564
GR/86/9	1.999	NA	1.25	445.87	3.075
GR/86/10	1.999	NA	1.25	445.87	3.075
GR/86/15	1.999	NA	2.50	332.51	2.293
GR/86/16	1.999	NA	1.25	404.30	2.788
GR/86/17	1.999	NA	1.25	272.05	1.876
GR/86/22	1.999	NA	2.50	294.72	2.033
GR/86/23	1.999	NA	1.25	396.74	2.736
GR/86/24	1.999	NA	1.25	392.97	2.710
Average				355.81	2.454

Table D-3. Point Load Index: Carlile Shale

Test	Platen Distance (inches)	Diameter of Core (inches)	1/2 Length of Core	Point Load Index $I_s(50)$	
				(psi)	(MPa)
AXIAL					
IG/86/1	1.055	2.962	NA	138.38	0.954
IG/86/2	1.402	2.955	NA	147.17	1.015
IG/86/3	1.637	2.953	NA	137.88	0.951
IG/86/4	1.585	2.946	NA	141.63	0.977
IG/86/5	1.540	2.984	NA	79.57	0.549
IG/86/6	1.765	2.948	NA	134.32	0.926
IG/86/7	2.936	2.965	NA	116.02	0.800
IG/86/8	1.700	2.983	NA	136.25	0.940
IG/86/9	1.202	2.995	NA	119.59	0.825
IG/86/16	1.330	2.953	NA	153.39	1.058
IG/86/17	2.026	2.940	NA	151.78	1.047
Average				132.36	0.913
DIAMETRAL					
IG/86/472-1	2.950	NA	2.5	56.84	0.392
IG/86/4-63	2.955	NA	2.1	32.99	0.227
IG/86/4-62	2.937	NA	2.7	49.53	0.342
IG/86/1-179	2.998	NA	2.0	9.88	0.068
IG/86/101	2.971	NA	3.3	43.96	0.303
IG/86/105	2.950	NA	4.7	101.29	0.699
IG/86/106A	2.948	NA	6.1	103.46	0.714
IG/86/106B	2.948	NA	3.2	156.44	1.079
IG/86/107A	2.947	NA	3.8	104.14	0.718
Average				73.17	0.505

Table D-4. Point Load Index: Chattanooga Shale

Test	Platen Distance (inches)	Diameter of Core (inches)	1/2 Length of Core	Point Load Index $I_s(50)$	
				(psi)	(MPa)
AXIAL					
CH/86/2C	0.660	1.422	NA	510.40	3.520
CH/86/2C3B	0.856	1.423	NA	468.16	3.229
Average				489.28	3.375
DIAMETRAL					
CH/86/2C3	1.423	NA	1.6	42.23	0.291
CH/86/2C2B	1.422	NA	0.6	51.25	0.353
Average				46.74	0.322

APPENDIX E

CREEP TESTS ON GREEN RIVER SPECIMENS

APPENDIX E
LIST OF FIGURES

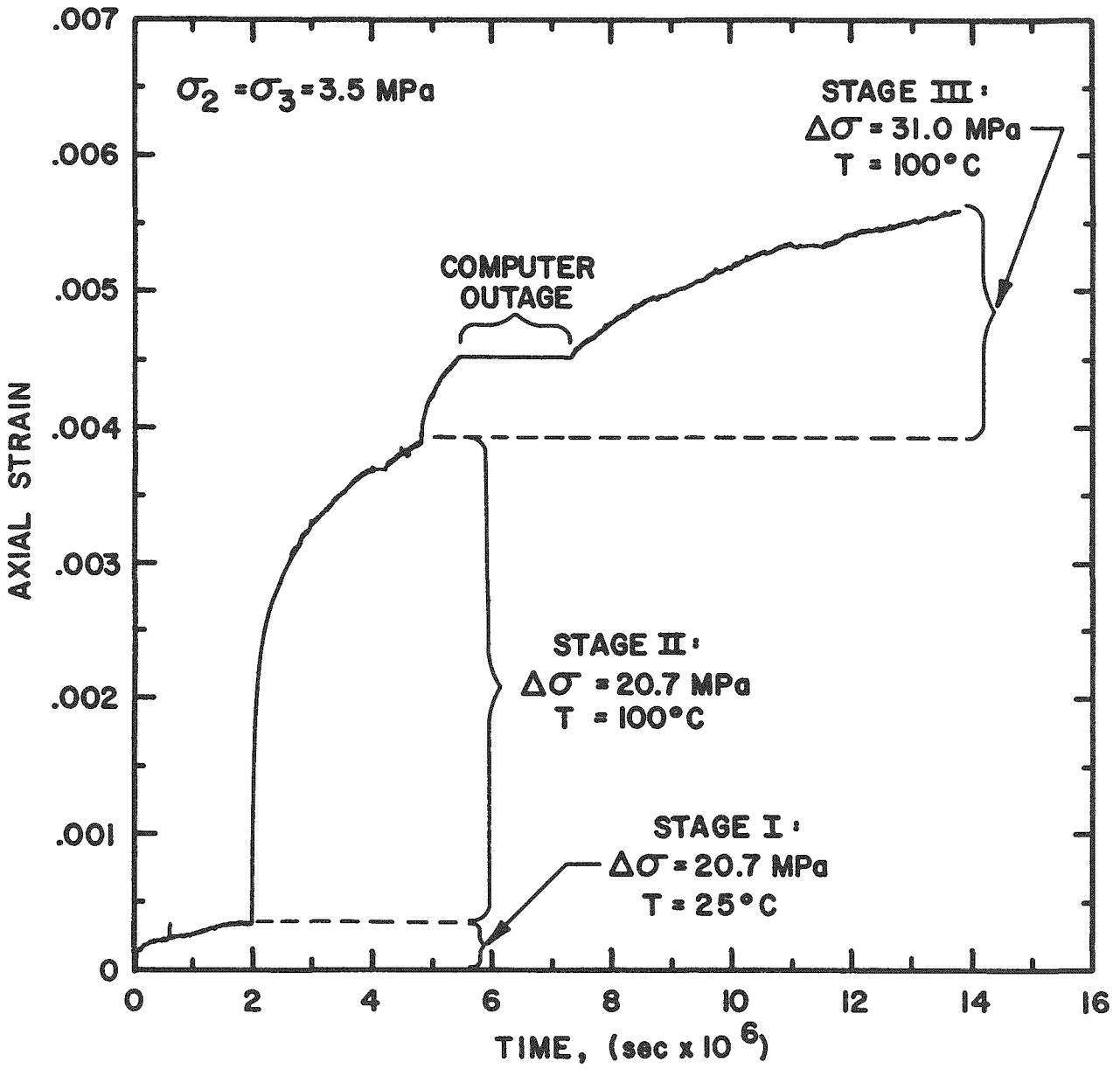

Figure E-1. Three-Stage Creep Test on Green River Specimen GR/86/V27-0/1-1/1

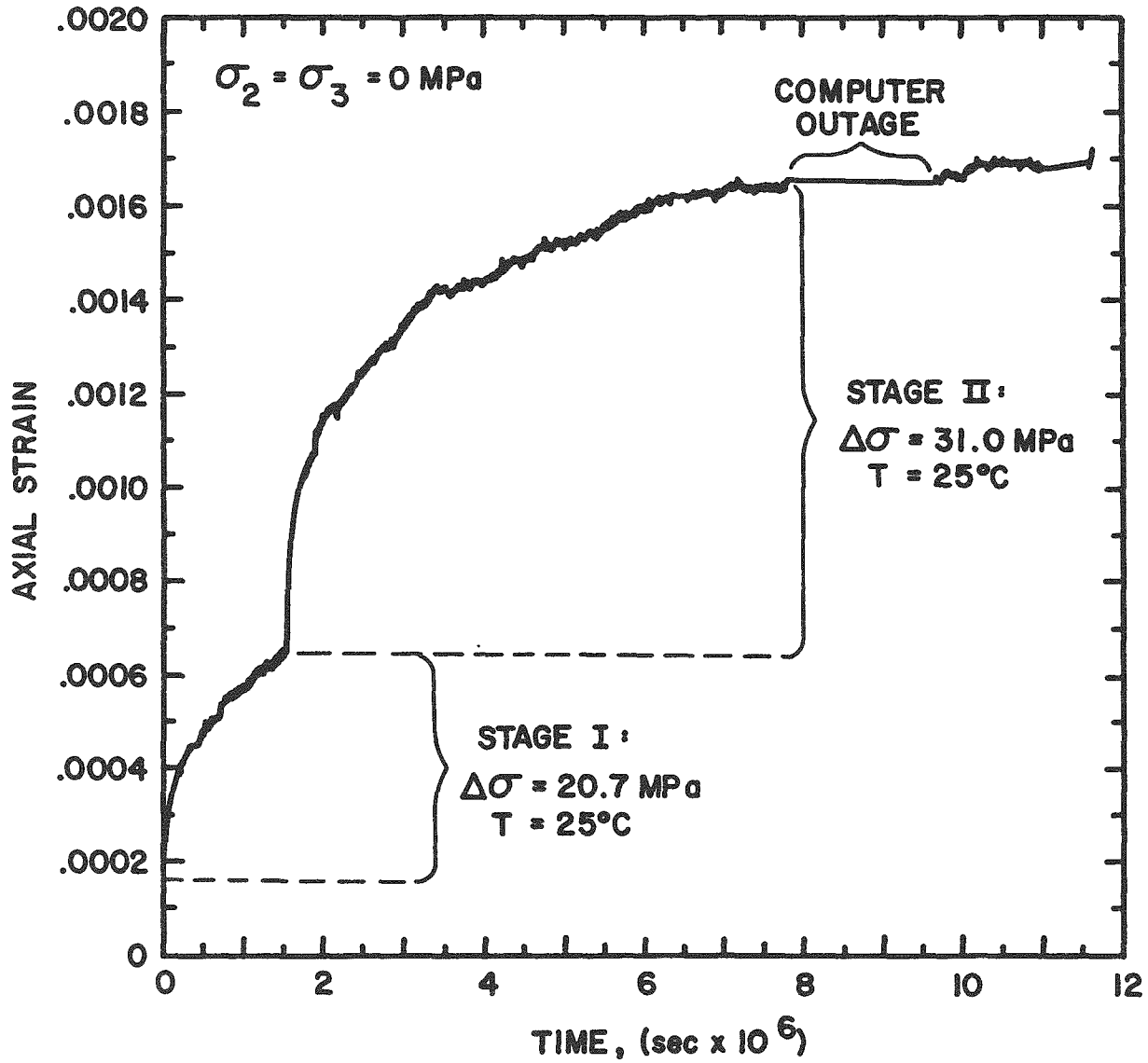

Figure E-2. Two-Stage Creep Test on Green River Specimen GR/86/V54-0/1-1/1

APPENDIX F

FREE SWELL OF SHALES

APPENDIX F
LIST OF FIGURES

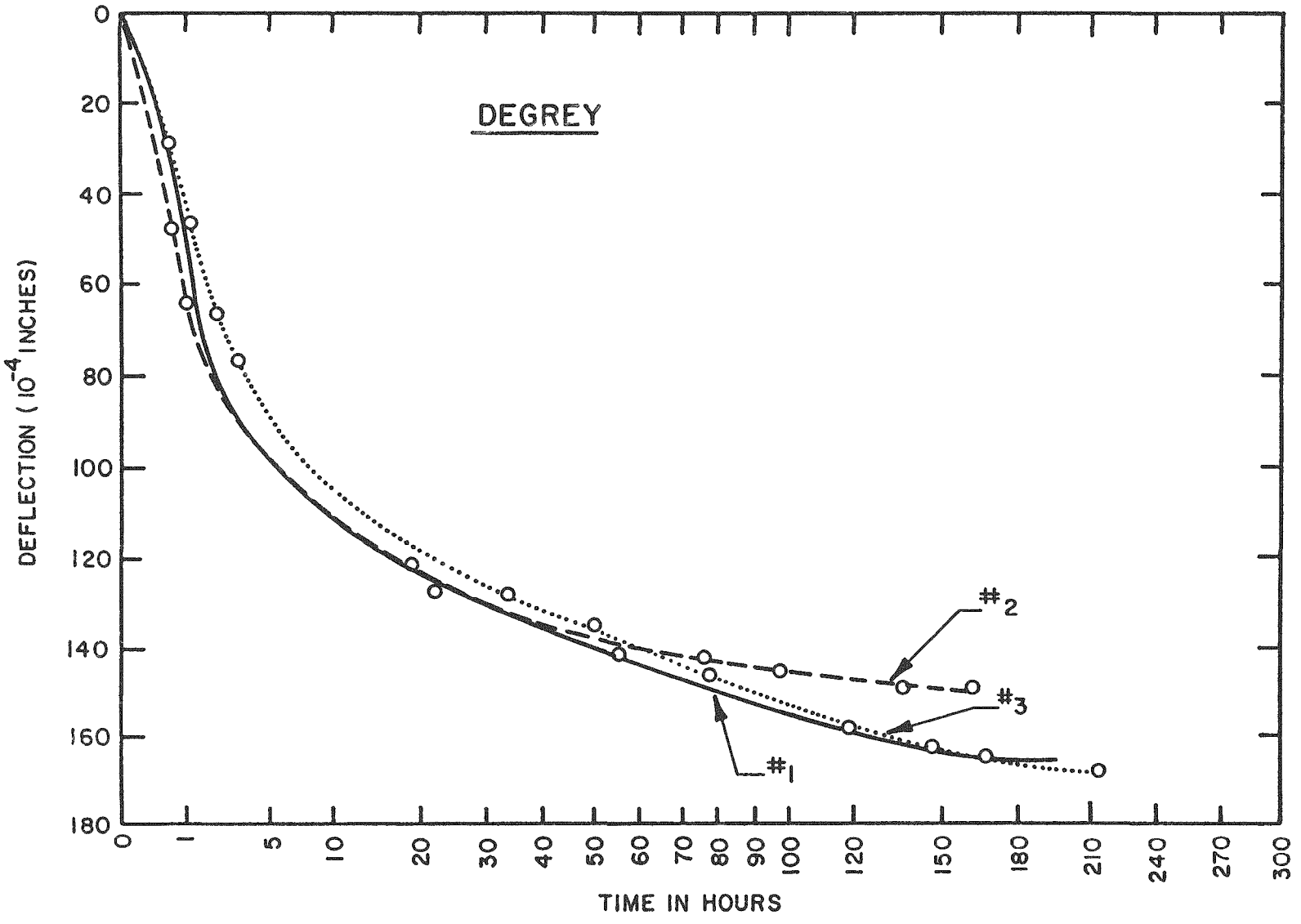

Figure F-1. Free Swell of the DeGrey Member of the Pierre Shale

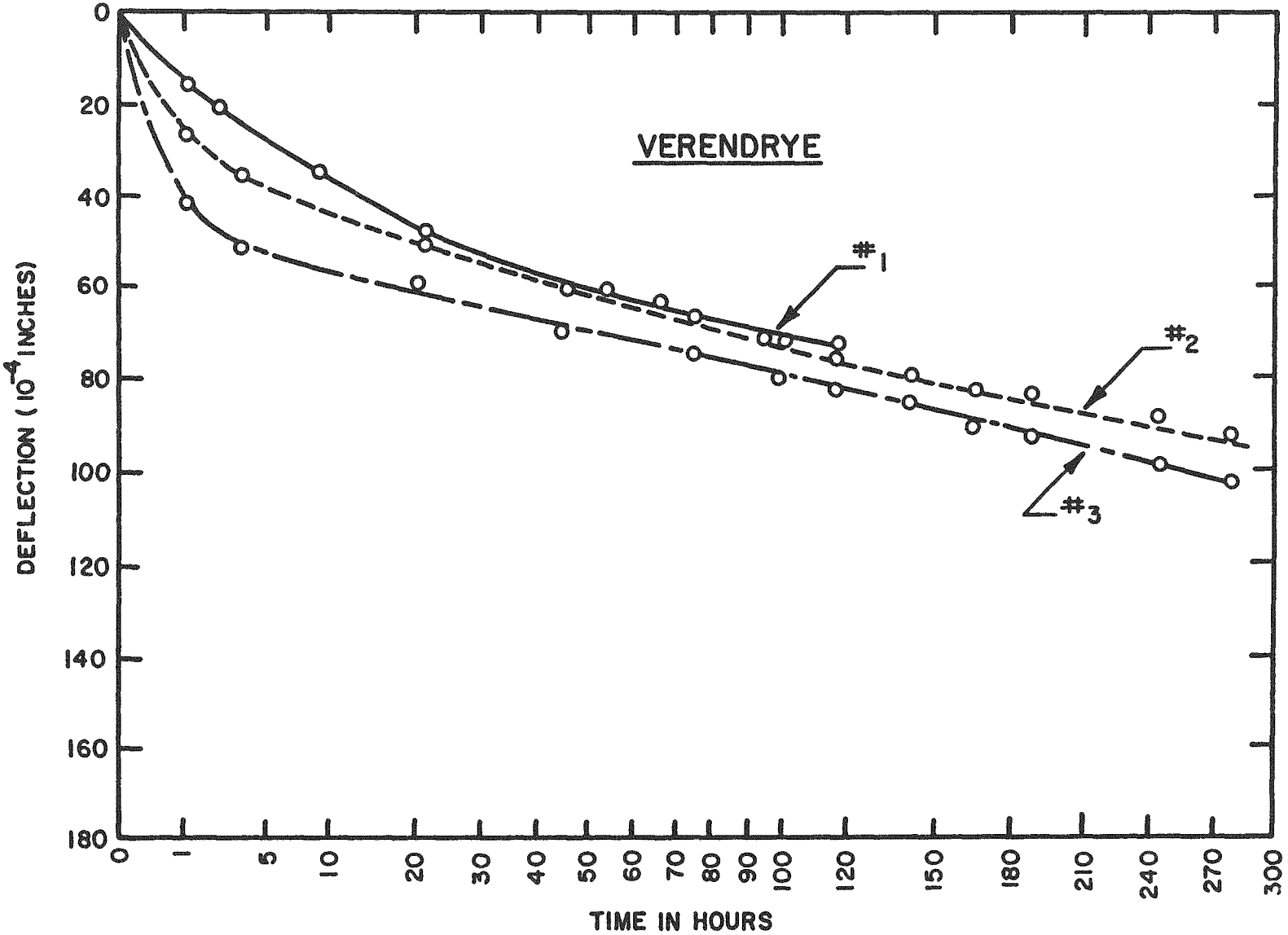

Figure F-2. Free Swell of the Verendrye Member of the Pierre Shale

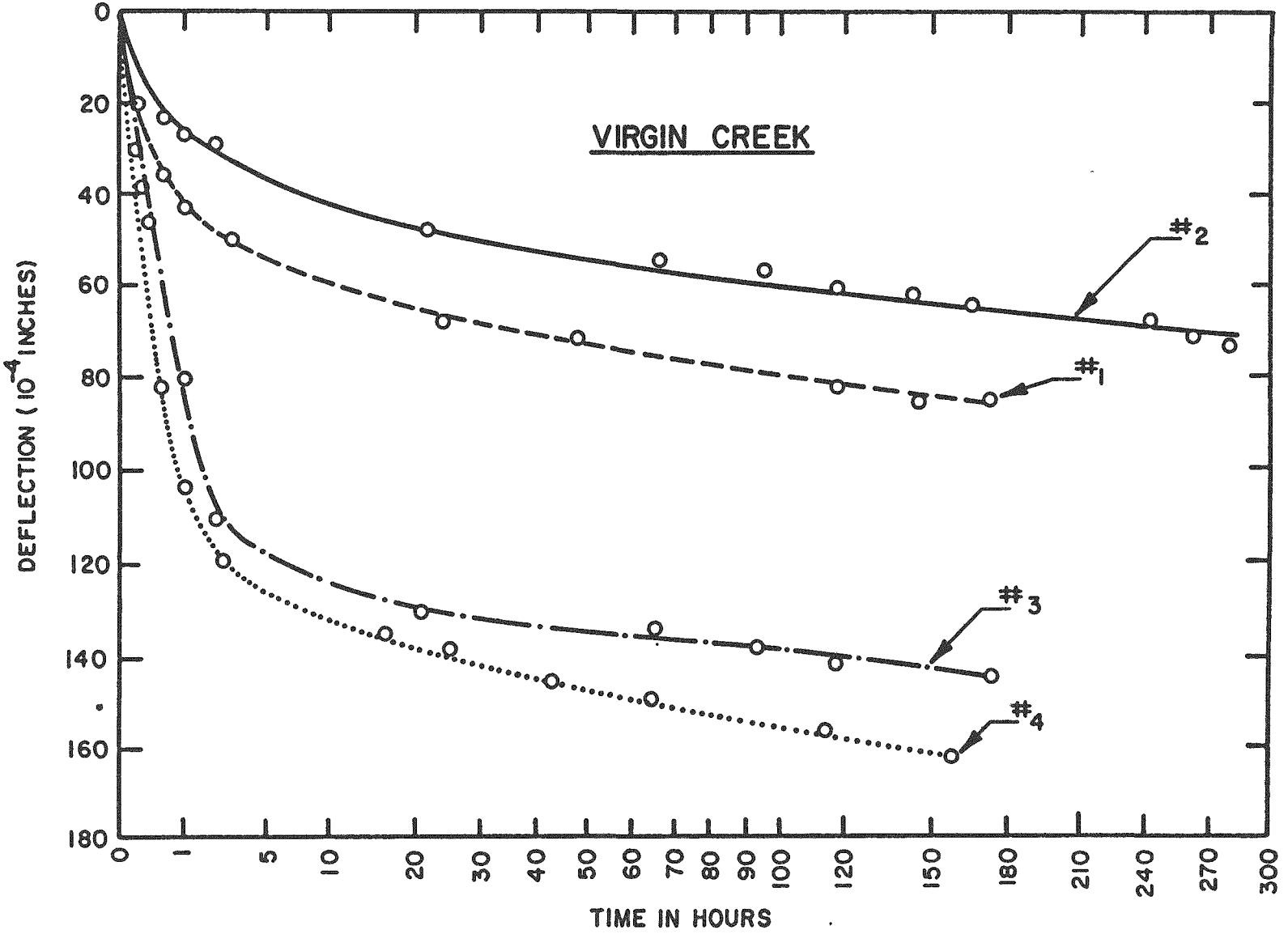

Figure F-3. Free Swell of the Virgin Creek Member of the Pierre Shale

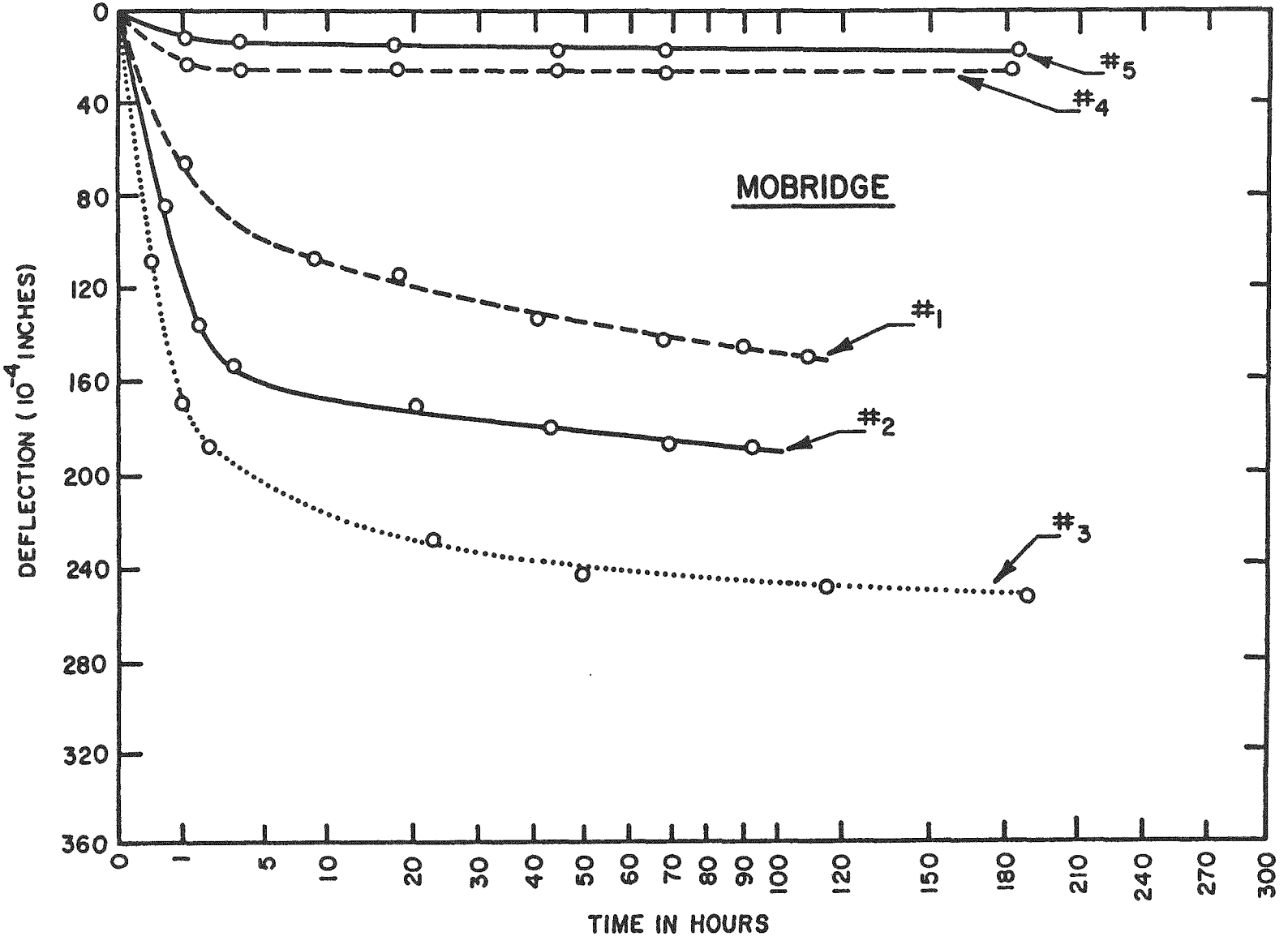

Figure F-4. Free Swell of the Mobridge Member of the Pierre Shale

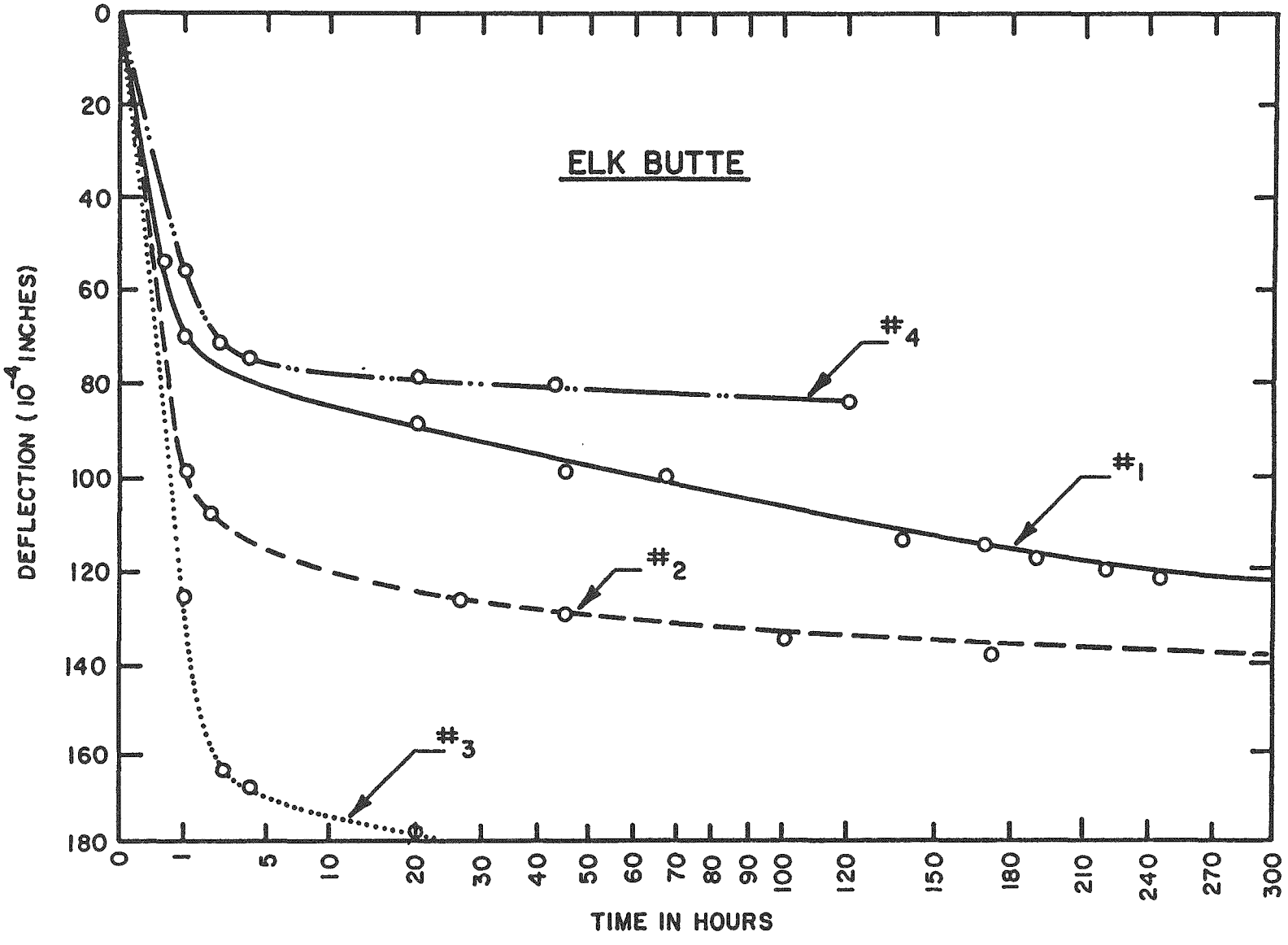

Figure F-5. Free Swell of the Elk Butte Member of the Pierre Shale

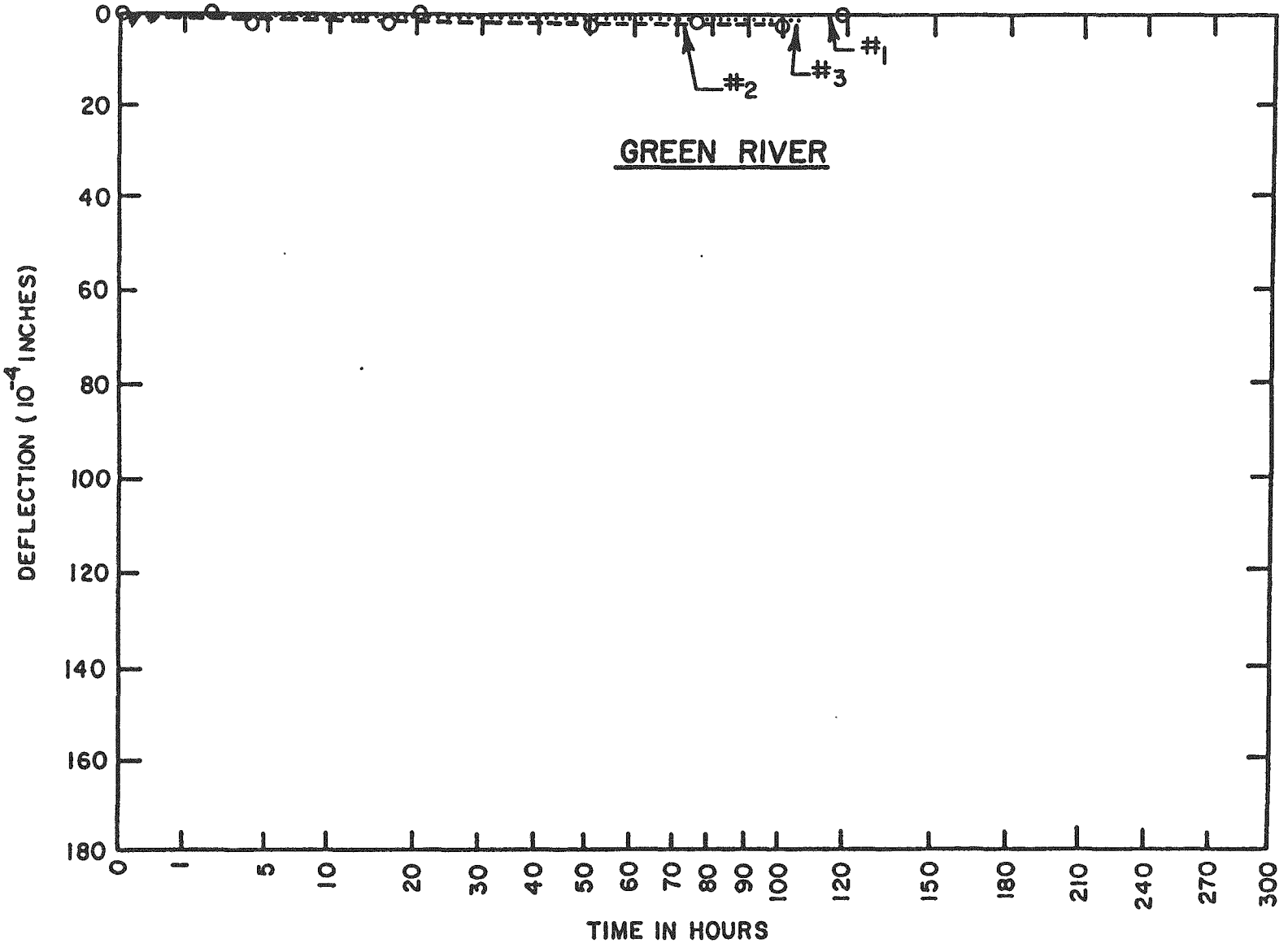

Figure F-6. Free Swell of the Green River Material

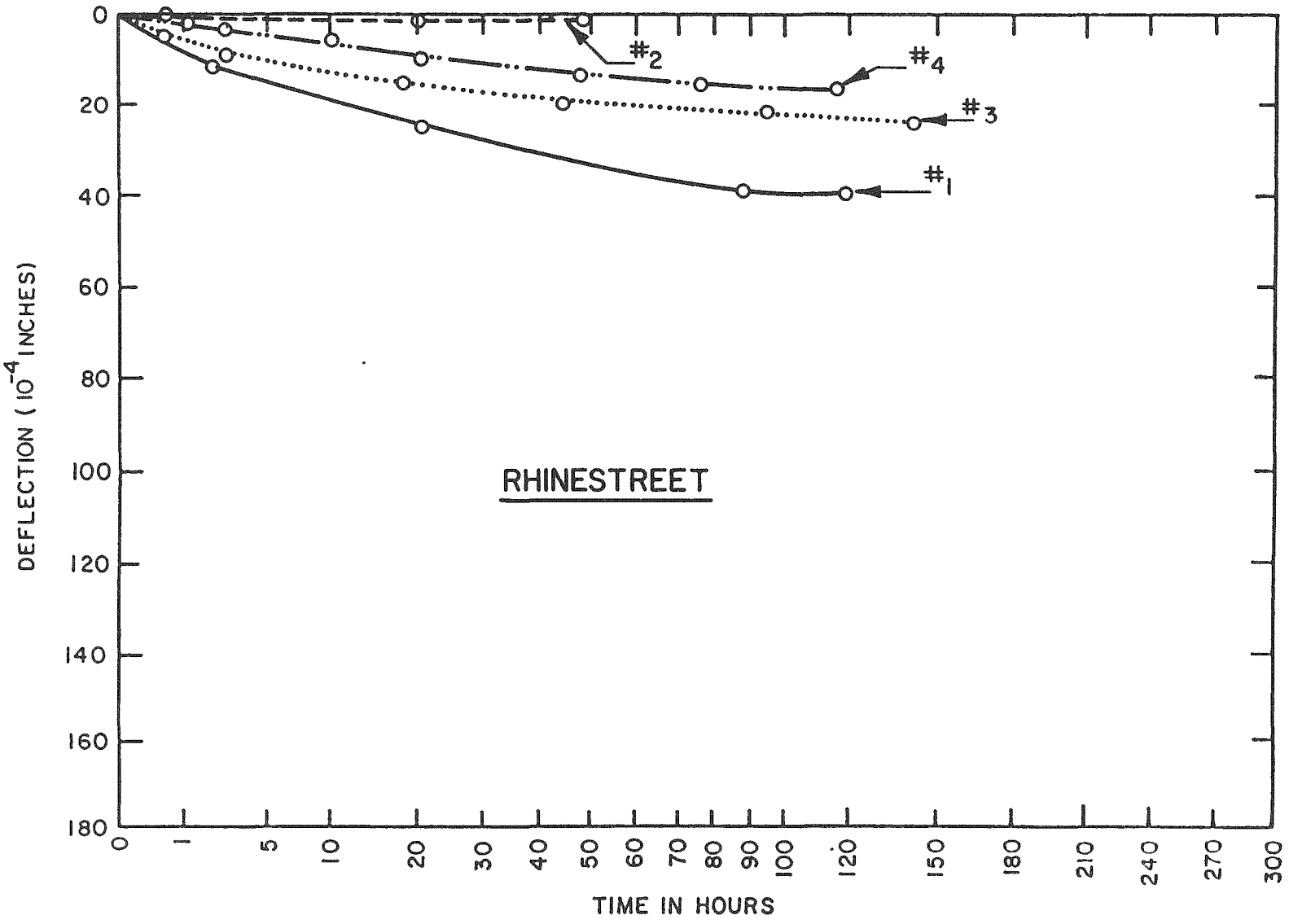

Figure F-7. Free Swell of the Rhinestreet Shale

ORNL/Sub/85-97343/2

INTERNAL DISTRIBUTION

1. A. G. Croff
2. R. B. Dreier
3. T. W. Hodge, Jr.
4. O. C. Kopp
5-9. T. F. Lomenick
10. T. H. Row
11. S. H. Stow
12. V. C. A. Vaughen
13. R. G. Wymer
14-15. Central Research Library
16-17. Laboratory Records
18. Laboratory Records — RC
19. ORNL Patent Section
20. ORNL Y-12 Technical Library, Document Reference Section

EXTERNAL DISTRIBUTION

21. Office of Assistant Manager for Energy Research and Development, Department of Energy, Civilian Radioactive Waste Management, 1000 Independence Ave., Washington, DC 20545
22. C. R. Cooley, Department of Energy, 1000 Independence Ave., Washington, DC 20545
23. S. H. Kale, Department of Energy, 1000 Independence Ave., Washington, DC 20545
24. R. C. Baker, Department of Energy, Chicago Operations Office, 9800 S. Cass Ave., Chicago, IL 60439
25. S. Mann, Department of Energy, Chicago Operations Office, 9800 S. Cass Ave., Chicago, IL 60439
26. J. D. Kasprowicz, Department of Energy, Chicago Operations Office, 9800 S. Cass Ave., Chicago, IL 60439
27. Neil Chapman, Institute of Geological Sciences, Exhibition Road, South Kensington, UK-London, SW72DE, United Kingdom
28. D. Gray, Institute of Geological Sciences, Exhibition Road, South Kensington, UK-London, SW72DE, United Kingdom
29. R. Heremans, National Agency for Radioactive Waste and Fissile Materials Mgt. ONDRAF/NIRAS, Boulevard du Regent 54-Boite 5, 1000 Brussels, Belgium
30. P. Manfroy, National Agency for Radioactive Waste and Fissile Materials Mgt. ONDRAF/NIRAS, Boulevard du Regent 54-Boite 5, 1000 Brussels, Belgium
31-33. W. E. Newcomb, Office of Waste Technology, Battelle Project Management Division, 7000 S. Adams St., Willowbrook, IL 60521
34. A. K. Yonk, Office of Waste Technology, Battelle Project Management Division, 7000 S. Adams St., Willowbrook, IL 60521

35. A. Fossom, RE/SPEC, Inc., P. O. Box 725, Rapid City, SD 57701
36. P. F. Gnirk, RE/SPEC, Inc., P. O. Box 725, Rapid City, SD 57701
37. F. D. Hansen, RE/SPEC, Inc., P. O. Box 725, Rapid City, SD 57701
38. M. Loken, RE/SPEC, Inc., P. O. Box 725, Rapid City, SD 57701
39. J. L. Ratigan, RE/SPEC, Inc., P. O. Box 725, Rapid City, SD 57701
40. T. J. Vogt, RE/SPEC, Inc., P. O. Box 725, Rapid City, SD 57701
41. N. L. Carter, Petroleum Engineering and Geophysics, Texas A&M University, College Station, TX 77843
42. P. A. Domenico, Petroleum Engineering and Geophysics, Texas A&M University, College Station, TX 77843
43. J. E. Russell, Petroleum Engineering and Geophysics, Texas A&M University, College Station, TX 77843
44. W. C. McClain, Roy F. Weston, Inc., 2301 Research Boulevard, Rockville, MD 20850
45. S. Panno, Roy F. Weston, Inc., 2301 Research Boulevard, Rockville, MD 20850
46. P. E. Ahlstrom, SKBF, Box 5864, S-102 48 Stockholm, Sweden
47. A. Barbreau, Commissariat a l'Energie Atomique, Inst de Protection et de Surete Nucleaire, Centre d'Etudes Nucleaires, B. P. No. 6, F-92260, Fontnay-Aux-Roses, France
48. Z. T. Bieniawski, Penn State University, University Park, PA 16802
49. A. Bonne, Belgian Nuclear Research Center, CEN/SCK, Boeretang 200, B.2400 Mol, Belgium
50. P. J. Bourke, UKAEA, B-151, Chem. Tech. Division, Atomic Energy Research Establishment, Harwell, GB-OXON, ORA, United Kingdom
51. W. Brewitz, Gesellschaft fur Strahlen und Umweltforschung mbH Munchen, Institut fur Tieflagerung, Wissenschafliche Abetilung, Theodorheusstrasse 4, D-3300 Braunschweig, FRG
52. D. Caldwell, Golder Associates, 2950 North Up Way, Bellevue, WA 98004
53. J. A. Cherry, Dept. of Earth Sciences, University of Waterloo, Waterloo, Ontario, Canada, N2L 3G1
54. J. O. Duguid, ICP Technology, 1850 K Street, N.W., Washington, DC 20006
55. Ferruccio Gera, Ismes Spa, 24100 Bergamo-Viale G. Cesare 29, Taramelli 14, 00197 Rome, Italy
56. S. Gonzales, Earth Resource Associates, Inc., 295 East Dougherty Street, Suite 105, Athens, GA 30601
57. J. Handin, 2614 Melba Circle, Bryan, TX 77892
58. D. Hansen, 2810-130 PL NE, Bellevue, WA 98005
59. M. P. Hardy, Agapito Associates, Inc., Suite 340, 715 Horizon Drive, Grand Junction, CO 81505
60. B. Y. Kanehiro, Berkeley Hydrotechnique, Inc., 2150 Shattuck Ave., Berkeley, CA 94704

61. K. Kuhn, Head of Institute, GSF, Berliner Strasse 2, D-3392 Clausthal-Zellerfeld, FRG
62. A. R. Lappin, Sandia National Laboratories, P. O. Box 5800, Albuquerque, NM 87185
63. W. G. Pariseau, University of Utah, Salt Lake City, UT 84112
64. Frank L. Parker, Vanderbilt University, Nashville, TN 37203
65. T. Pigford, Dept. of Nuclear Engineering, College of Engineering, University of California, Berkeley, CA 94720
66. P. E. Potter, Department of Geology, University of Cincinnati, Cincinnati, OH 45221
67. Atou Shimozato, Nuclear Power Generation Division, Hitachi, Ltd., 6 Kanda-Surugadai 4 Chome, Chiyoda-Ku, Tokyo 01, Japan
68. H. W. Smedes, 1126 Buehler Dr., Las Vegas, NV 89102
69. P. R. Stevens, Department of the Interior, U.S. Geological Survey, Reston, VA 22092
70. H. S. Swolfs, Department of the Interior, U.S. Geological Survey, Federal Center, Denver, CO 80225
71. K. T. Thomas, Waste Management Section, Division of Nuclear Fuel Cycle, International Atomic Energy Agency, Wagramerstrasse 5, P. O. Box 200, A-1400 Vienna, Austria
72. M. F. Thury, NAGRA-National Cooperative for the Storage of Radioactive Waste, Parkstrasse 23, CH-5401 Baden, Switzerland
73. W. S. Twenhofel, 820 Estes Street, Lakewood, CO 80215
74. P. Venet, Commission of the European Communities, Directorate General XII, Nuclear Fuel Cycle Division, 200 Rue de la Loi, B-1040 Brussels, Belgium
75. S. H. Whitaker, Applied Geoscience Branch, Atomic Energy of Canada, Ltd., Whiteshell Nuclear Research Establishment, Pinawa, Manitoba ROE 1 LO, Canada

76-105. Technical Information Center, Oak Ridge, TN 37831

106. Office of Assistant Manager, Energy Research and Development, DOE-ORO, Oak Ridge, TN 37831